541

Copy
RM E57C12a

[redacted]

DECLASSIFIED

NACA

RESEARCH MEMORANDUM

INVESTIGATION OF HIGH-ANGLE-OF-ATTACK PERFORMANCE OF A 14° RAMP-TYPE INLET IN VARIOUS CIRCUMFERENTIAL BODY LOCATIONS

MACH NUMBER RANGE 1.5 TO 2.0

By Glenn A. Mitchell and Bruce G. Chiccine

Lewis Flight Propulsion Laboratory
Cleveland, Ohio

Declassified by authority of NASA
Classification Change Notices No. 67
Dated ** 6/29/66

DECLASSIFIED- AUTHORITY
US: 1286 DROBKA TO LEBOW
MEMO DATED 6/8/66

[redacted]

NATIONAL ADVISORY COMMITTEE
FOR AERONAUTICS

WASHINGTON

June 26, 1957

[redacted]

 CONFIDENTIAL DECLASSIFIED

NATIONAL ADVISORY COMMITTEE FOR AERONAUTICS

RESEARCH MEMORANDUM

INVESTIGATION OF HIGH-ANGLE-OF-ATTACK PERFORMANCE OF A 14° RAMP-TYPE INLET IN VARIOUS CIRCUMFERENTIAL BODY LOCATIONS

MACH NUMBER RANGE 1.5 TO 2.0

By Glenn A. Mitchell and Bruce G. Chiccine

SUMMARY

An experimental investigation to determine the internal flow performance of a fixed 14° ramp inlet from zero to 20° angle of attack was conducted at free-stream Mach numbers of 1.5, 1.8, and 2.0. The inlet was mounted in three circumferential fuselage locations and utilized inlet throat and fuselage boundary-layer removal.

Results indicate a superiority of a bottom inlet location over a side or top inlet location at angles of attack; relatively low pressure recoveries and high distortions were obtained with side and top inlets. Some improvement in side inlet performance was obtained with the use of flow deflector plates mounted at the top side of the inlet. Improvements in top inlet performance resulted from the substitution of a rounded approach for the original flat approach to the inlet. Distortion levels for these modifications to the original side and top inlet configurations remained prohibitively high. However, placing a canopy in front of the top inlet, although decreasing the performance at low angles of attack, improved pressure recovery and greatly reduced distortions at higher angles.

INTRODUCTION

Past research has shown that body crossflow phenomena and variable boundary-layer thickness along the circumference of a fuselage at angles of attack have significant effects on the angle-of-attack performance of an inlet in various circumferential locations (refs. 1 to 4). Specifically, pressure recovery performance for bottom inlet locations was maintained up to the highest angles of attack tested, 10° to 12°, whereas sizable reductions in pressure recovery were incurred by side and top inlets. The performance of these inlets was obtained with fuselage boundary-layer removal generally adequate for the case at zero angle of attack.

[redacted]

More recent investigations (such as ref. 5) with aft inlets utilizing fuselage boundary-layer removal have indicated increased performance at zero angle of attack by bleeding off boundary layer in the vicinity of the inlet throat. With proper throat bleed this performance gain could be maintained independently of the amount of fuselage boundary-layer removal. As an extension of this work, a study was conducted to determine if the beneficial effects of bleed could be extended to the case of aft inlets at angles of attack. A fixed 14° ramp inlet with fuselage and inlet throat boundary-layer removal was tested alternately in the bottom, side, and top positions on a body of revolution in the 8- by 6-foot supersonic wind tunnel at Mach numbers of 1.5, 1.8, and 2.0 and angles of attack from zero to 20°.

SYMBOLS

A	area, sq in.
A_B	bleed minimum exit area, sq in.
A_i	inlet capture area, 19.51 sq in.
A_t	inlet throat area, 13.55 sq in.
A_2	diffuser flow area at model station 85.0, 18.31 sq in.
A_3	diffuser flow area at model station 99.2, 22.99 sq in.
D_h	hydraulic diameter, $\frac{4A}{\text{wetted perimeter}}$
h	fuselage boundary-layer diverter height, in.
M	Mach number
m_3/m_0	main-duct mass-flow ratio, $\frac{\text{main-duct mass flow}}{\rho_0 V_0 A_i}$.
$\Delta(m_3/m_0)$	stable range of mass-flow ratio, $(m_3/m_0)_{cr} - (m_3/m_0)_{min\ stable}$
P	total pressure
P_1	measured total pressure (pitot pressure) at boundary-layer survey station
$\frac{P_{2,max} - P_{2,min}}{P_2}$	total-pressure distortion
$P_{2,max} - P_{2,min}$	maximum total-pressure variation at pressure rake at model station 85.0

t	fuselage boundary-layer thickness at zero angle of attack (0.55 in. at model station 55.1)
V	velocity, ft/sec
$\frac{w\sqrt{\theta}}{\delta A}$	weight flow per unit area, referenced to standard sea-level conditions, (lb/sec)(sq ft)
α	angle of attack, deg
δ	ratio of total pressure to NACA standard sea-level total pressure of 2116.22 lb/sq ft
θ	ratio of total temperature to NACA standard sea-level temperature of 518.688° R
ρ	mass density

Subscripts:

cr	critical
max	maximum
min	minimum
0	free stream
1	fuselage boundary-layer survey station, model station 55.1
2	diffuser total-pressure survey station, model station 85.0
3	diffuser static-pressure survey station, model station 99.2

APPARATUS AND PROCEDURE

A schematic drawing of the fuselage, inlet, and boundary-layer removal system of the bottom inlet configuration is presented in figure 1, and a photograph of the inlet appears in figure 2. Photographs of the side and top inlet configurations are shown in figures 3 and 4. The inlet-diffuser assembly was mounted, with one exception, on the flat side of a basic body-of-revolution consisting of an ogive nose and a 10-inch-diameter cylindrical afterbody aft of model station 46.2. For the

exception (fig. 4(b)) the flat was eliminated and the inlet was mounted directly on the cylindrical body. In the other top inlet configurations (figs. 4(a) and (c)) the inlet was mounted on the flat. The inlet cowl lip for all configurations was located at model station 61.9. Swept side fairings, used on the inlet, extended from the cowl sides to the leading edge of the ramp.

Fuselage boundary-layer diverter height was varied with spacers inserted between the body and the inlet-diffuser installation. Two diverter heights were investigated, 0.183 and 0.55 inch ($h/t = 1/3$ and 1). In the top inlet configuration with the inlet mounted on the cylindrical body, the diverter height was 0.55 inch only on the vertical center plane. The diffuser reference line was maintained parallel to the body axis at all times.

Boundary layer entering the inlet of the bottom and side inlet configurations was removed by a flush slot located on the compression ramp inside the inlet and extending from wall to wall. Mass flow drawn through this slot and dumped into the bleed chamber was ejected through openings in either side of the inlet cowl. Variation in bleed mass flow was accomplished by varying back pressure in the bleed chamber with a pair of remotely controlled doors at the bleed exits.

Except for details of the bleed system, the inlet was identical to that reported in reference 5. The flush slot bleed system of reference 5 does not have a bleed chamber such as shown in figure 1 but has a smoothly faired duct from the slot to the bleed exit. The slot area of the present configuration was 4.48 square inches; that of reference 5 was 4.25 square inches.

The top inlet configurations had, in addition to the flush slot, ramp perforations lying almost wholly forward of the cowl lip. The open area of the perforations was 2.5 square inches or 18.4 percent of the throat area, and the porosity of this perforated area was 24 percent (hole diam., 0.07 in.; plate thickness, 0.12 in.). Both the flush slot and the perforations were open to the same bleed chamber. In an attempt to provide additional bleed exit area, slots were cut into the sides of the ramp and vents were added as shown in figure 4(a).

The flow deflector plates used with the side inlet (figs. 3(b) and (c)) were mounted 0.25 inch from the side of the ramp and extended forward of the ramp leading edge 3.64 and 8.39 inches or 76 and 154 percent of the inlet width for the short and long deflector plates, respectively.

The diffuser area variation is shown in figure 5. The area decrease at a point about 20 inches downstream of the cowl lip is due to the presence of the centerbody shown in figure 1.

The model was connected directly to the support sting. Data were taken in two angle-of-attack ranges. Angle-of-attack data from zero to 8.6° were obtained with a straight sting; a skewed flange aft of the model was used to provide a range of angle of attack of 8.6° to 20°. Inlet mass flow was varied by means of a remotely controlled movable tailpipe plug attached to the sting.

The flow field ahead of the inlet was determined from a survey rake at model station 55.1. The average total pressure at the diffuser exit was obtained from an area-weighted average of 32 total-pressure tubes located at station 85.0. The tubes were arranged in eight rakes equally spaced around the diffuser centerbody. The static-pressure orifices at station 85.0 were located both on the centerbody and the diffuser wall. Main duct mass-flow ratio was determined from the six static-pressure orifices (equally spaced around the diffuser wall) at station 99.2 and the known area ratio between that station and the exit plug where the flow was assumed to be choked.

Inlet stability was determined from oscillographs of a pressure transducer located in the diffuser at model station 85.0. The limit of stability, or the minimum stable point, of inlet operation was defined as a static-pressure pulsation with an amplitude of 5 percent of the diffuser total pressure.

The model was tested with the inlet in three circumferential locations at angles of attack from zero to 20° and at free-stream Mach numbers of 1.5, 1.8, and 2.0. The configurations investigated are listed in the following table:

Configuration	Bleed system	Side fairings	Fuselage diverter height parameter, h/t
Bottom inlet	Flush slot	On	1, 1/3
Side inlet	Flush slot	Off	1
Side inlet with short deflector plate	Flush slot	Off	1
Side inlet with long deflector plate	Flush slot	Off	1
Top inlet	Flush slot and ramp perforations	On	1
Top inlet with rounded approach	Flush slot and ramp perforations	On	[a]1
Top inlet with canopy	Flush slot and ramp perforations	On	1

[a]Value of h measured at [redacted] plane.

RESULTS AND DISCUSSION

Survey of Body Flow Field

Measured total-pressure profiles ahead of the inlet station for some of the configurations investigated are presented in figure 6. (The profiles shown in fig. 6(a) for a rounded approach on top of the body were obtained with the flat on the bottom of the body.) Outside of the boundary layer, flat or uniform profiles over the complete range of angle of attack were obtained only on the bottom of the body (fig. 6(b)). The flat profiles obtained on the top of the body up to an angle of attack of 14° (fig. 6(a)) may be misleading in that variations in total pressure across the span of the inlet due to crossflow effects and boundary-layer thickening (ref. 2) could affect the performance of an inlet situated in this top position. Figures 6(c) and (d) show the development of low-energy regions on the side of the body leading to separation at an angle of attack of about 20°.

Variation of boundary-layer thickness on the flat bottom of the fuselage with angle of attack is shown in figure 7 for free-stream Mach numbers of 1.5, 1.8, and 2.0. The major decrease in boundary-layer thickness occurred at angles of attack between zero and 8°. At an angle of attack of 8° the boundary-layer thickness was about 55 percent of the thickness at zero angle of attack. The zero-angle-of-attack boundary-layer thickness of 0.55 inch was obtained from reference 5.

Bottom Inlet Configuration: Flush Slot Bleed and Inlet Side Fairings

Inlet performance characteristics (total-pressure recovery and distortions) at zero angle of attack for the bottom inlet with full fuselage boundary-layer removal ($h/t = 1$) are presented in figure 8. The data are plotted as a function of the main-duct mass-flow ratio for several values of bleed exit area. Both total-pressure recovery and distortion were improved by bleeding at the inlet throat as reported in reference 5. The pressure recovery levels of this configuration were similar to those of the flush slot bleed configuration of reference 5. However, a rather large decrease in critical mass-flow ratio with increasing inlet throat bleed was reported in reference 5 while the present configuration exhibited only small decreases with bleed. Evidently, the present configuration had a very low supercritical flow coefficient through the bleed system. The similarity of performance of the two configurations suggests that the subcritical flow coefficients were about the same.

The angle-of-attack performance was obtained with a fixed bleed door position of $A_B/A_t = 0.155$ which corresponded to the value shown

in reference 5 to provide nearly optimum pressure recovery and thrust-minus-drag. Angle-of-attack performance for the bottom inlet configuration with a fuselage diverter height equal to the boundary-layer thickness at zero angle of attack is presented in figure 9(a). Peak pressure recovery at each free-stream Mach number varied only 2 percent over the range of angles of attack up to 20°. Reduction in peak recovery with angle of attack occurred only at a free-stream Mach number of 1.8. An increase in both peak and critical pressure recovery was observed at a free-stream Mach number of 2.0. Total-pressure distortions at critical mass-flow ratio were below 15 percent at angles of attack from zero to 20°.

If the inlet was operated at the corrected weight flow which appears to give optimum performance at zero angle of attack $\left(\frac{w\sqrt{\theta}}{\delta A} \approx 25\right.$ at $\left.M_0 = 2.0\right)$, angle-of-attack operation would make the inlet slightly more subcritical. With this type of inlet operation total-pressure recovery would vary less than 2 percent and distortions would remain below 15 percent over the angle-of-attack range.

The range of stable mass-flow ratio increased with angle of attack. At a free-stream Mach number of 2.0 the range of stable mass-flow ratio increased from 0.05 at zero angle of attack to at least 0.69 at an angle of attack of 20° (fig. 9(a)).

Reduction of the fuselage diverter height to one-third the boundary-layer thickness at zero angle of attack (fig. 9(b)) resulted in performance that was practically identical to the performance of the inlet with complete boundary-layer removal. These data corroborate somewhat those of reference 5 where at zero angle of attack it was found that, with sufficient inlet throat bleed, inlet peak pressure recovery is relatively insensitive to boundary-layer diverter height.

Side Inlet Configuration: Flush Slot Bleed and No Inlet Side Fairings

The angle-of-attack performance of the side inlet configurations (basic configuration or inlet with no deflector, inlet with short deflector, and inlet with long deflector) is presented in figure 10. The performance of the three configurations is compared with that of the bottom inlet in figure 11. The comparisons are made at selected values of corrected weight flow which appear to be those for nearly optimum performance of the side inlet at zero angle of attack. Large decreases in pressure recovery and increases in distortion with angle of attack were observed for all three side inlet configurations. At a free-stream Mach number of 2.0 peak pressure recovery dropped from a value of 0.87 at zero angle of attack to about 0.50 at an angle of attack of 20°.

[redacted]

Total-pressure distortions at critical mass-flow ratio were generally in excess of 50 percent at an angle of attack of 20° for all free-stream Mach numbers.

The differences in performance between the bottom and side inlets at zero angle of attack result from the fact that side fairings were not used on the side inlet configurations. (These were omitted because of possible detrimental effects at angle of attack in the presence of body crossflow.) The effects of removing the side fairings (at zero angle of attack) were typical (ref. 6) in that pressure recovery and mass-flow ratio were decreased (distortion was decreased slightly also) while stability was somewhat increased.

The flow deflector plates (examined only in the angle-of-attack range from 8.6° to 20°) produced significant improvements in peak pressure recovery (6 to 8 percent) only at a free-stream Mach number of 2.0 and an angle of attack of 8.6°. Here the deflector plates maintained peak recovery within 2 to 4 percent of the peak recovery at zero angle of attack.

Operation of the inlet along the selected match lines (fig. 11) generally caused the basic configuration to become supercritical as angle of attack was increased. However, inlet operation went subcritical at angle of attack for both configurations with a deflector plate. This shift to more subcritical operation generally lowered the distortion at a free-stream Mach number of 2.0. The use of the deflector plates consistently lowered critical distortions only at a free-stream Mach number of 1.5.

In general, the stability range of the side inlet configurations decreased as the angle of attack was increased. At the higher angles of attack the basic configuration had almost no stability. Both flow deflector plates were able to improve the stability, but the greatest improvement was obtained with the long deflector plate which had a stable mass-flow range of about 0.20 at an angle of attack of 20° (fig. 11). In contrast to the bottom inlet performance, if the side inlets were controlled to operate at a constant corrected weight flow, the inlet may be forced into buzz at angles of attack, depending on the match line selected.

Top Inlet Configuration: Flush Slot and Ramp

Perforations with Inlet Side Fairings

The inlet configuration tested in the bottom position had a relatively small stable range at zero angle of attack. It was felt that an inlet having a potential for greater stability was necessary for the top fuselage position. Previous work (such as ref. 7) has shown stability

improvement with the use of perforations on the compression surface ahead of the inlet. Accordingly, the top inlet configuration was modified to include the perforated ramp as well as the flush slot at the throat. Vents were cut into the sides of the ramp (fig. 4(a)) to provide additional bleed exit area which would be in close proximity to the perforations.

The performance of the combined ramp- and throat-bleed configuration is shown in figure 12 at zero angle of attack for varying amounts of bleed flow. The minimum bleed value A_B/A_t of 0.130 represents bleed through vents only (bleed doors closed); higher values indicate opening of the bleed doors toward the maximum position. Schlieren observation showed that, over a large part of the subcritical range, reverse flow occurred through the forward rows of the perforations even at the maximum bleed door opening. Despite this, peak pressure recovery and distortion levels were comparable to those obtained with throat bleed alone (fig. 8), although critical recovery decreased somewhat. Inlet stability was approximately doubled to a maximum value of about 20 percent of the critical mass flow.

The performance of the top inlet configurations at angle of attack is shown in figure 13, and performance comparisons are made in figure 14 at the same values of corrected weight flow selected for the side inlets. (In some instances data were obtained only in the range of angles of attack from 8.6° to 20°.) For these configurations the bleed flow ratios A_B/A_t include a value of 0.130 which represents bleed through the vents alone. Data for the top inlet configurations (basic configuration or flat approach to the inlet, rounded approach, and flat approach with canopy) were obtained at an A_B/A_t of 0.285. Limited data at an A_B/A_t of 0.595 with the flat approach to the inlet (fig. 13(b)) showed no improvement in performance with this increased bleed exit area.

As with the side inlet, large decreases in pressure recovery resulted from increased angle of attack. At a free-stream Mach number of 2.0 peak pressure recovery dropped from a value of 0.91 for the basic configuration at zero angle of attack to values of 0.50 to 0.55 for all configurations at an angle of attack of 20°. Distortions of the basic configuration were high at the intermediate angles of attack (28 to 37 percent) but dropped to values near 15 percent at an angle of attack of 20° (fig. 14).

Significant gains in pressure recovery at all Mach numbers and angles of attack were obtained by the substitution of a rounded for a flat approach to the inlet (fig. 14). Distortions were reduced but remained relatively high, generally over 20 percent at the intermediate angles of attack. These performance improvements were in part due to better

streamlining in the direction of crossflow and in part to the greater boundary-layer removal capabilities of the rounded approach which had an h/t as small as 1 only in the vertical center plane.

The use of a canopy in front of the inlet with the flat approach adversely affected pressure recovery and distortion at low angles of attack (less than 4°). However, at higher angles of attack pressure recovery was improved somewhat and very large gains were made in reducing distortion; for example, at a free-stream Mach number of 2.0 and an angle of attack of 14°, distortion decreased from 37 to 7 percent (fig. 14).

Figure 13 illustrates that the top inlet configurations, when operated at a constant corrected weight flow, are forced into a more subcritical operation by angle of attack without generally being forced into buzz as were the side inlets. The stability of the top inlet configurations was generally maintained with angle of attack at a mass-flow ratio range of 0.20 to 0.40. In some instances, however, the stability decreased to a mass-flow ratio range of 0.10 or less at the intermediate angles of attack.

SUMMARY OF RESULTS

An experimental investigation to determine the total-pressure recovery, distortion, and stability up to an angle of attack of 20° of a 14° ramp-type inlet with throat bleed and located in three circumferential fuselage positions was conducted in the Lewis 8- by 6-foot supersonic wind tunnel at free-stream Mach numbers of 1.5, 1.8, and 2.0. The following results were obtained:

1. The angle-of-attack performance of the bottom inlet was superior to that of the side and top inlet configurations. Up to an angle of attack of 20°, peak total-pressure recovery of the bottom inlet varied less than 2 percent, distortions were below 15 percent, and the stable mass-flow ratio range increased to values as large as 0.69. This angle-of-attack performance was maintained with the fuselage diverter height reduced to one-third the boundary-layer thickness at zero angle of attack.

2. Angle of attack reduced peak pressure recoveries of all side inlet configurations to values near 0.50 at an angle of attack of 20° and a free-stream Mach number of 2.0 and increased critical distortions to values in excess of 50 percent. The configurations with a flow deflector plate produced significant improvements in peak pressure recovery (6 to 8 percent) only at a free-stream Mach number of 2.0 and an angle of attack of 8.6°.

[redacted]

3. The pressure recoveries of the top inlet configurations were also reduced with angle of attack to values near 0.50 at an angle of attack of 20° and a free-stream Mach number of 2.0. The distortion of the top inlet with flat approach was high (28 to 37 percent) at the intermediate angles of attack but at an angle of attack of 20° dropped to about 15 percent or less. The substitution of a rounded for a flat approach to the inlet improved pressure recovery and distortions, but distortions were still relatively high, generally in excess of 20 percent.

4. Placing a canopy in front of the top inlet with the flat approach decreased pressure recovery and increased distortions at low angles of attack. However, at higher angles of attack the canopy improved the pressure recovery somewhat and greatly reduced distortions.

5. At selected engine match conditions (constant corrected weight flow close to optimum thrust-minus-drag at zero angle of attack) the top and bottom inlet configurations were forced subcritical and the side inlet was forced supercritical with angle of attack. With the use of flow deflector plates side inlet operation at these same weight flows was subcritical over the entire range of angle of attack.

Lewis Flight Propulsion Laboratory
National Advisory Committee for Aeronautics
Cleveland, Ohio, March 19, 1957

REFERENCES

1. Kremzier, Emil J., and Campbell, Robert C.: Angle-of-Attack Supersonic Performance of a Configuration Consisting of a Ramp-Type Scoop Inlet Located Either on Top or Bottom of a Body of Revolution. NACA RM E54C09, 1954.

2. Valerino, Alfred S., Pennington, Donald B., and Vargo, Donald J.: Effect of Circumferential Location on Angle of Attack Performance of Twin Half-Conical Scoop-Type Inlets Mounted Symmetrically on the RM-10 Body of Revolution. NACA RM E53G09, 1953.

3. Hasel, Lowell E., Lankford, John L., and Robins, A. W.: Investigation of a Half-Conical Scoop Inlet Mounted at Five Alternate Circumferential Locations Around a Circular Fuselage. Pressure-Recovery Results at a Mach Number of 2.01. NACA RM L53D30b, 1953.

4. Hasel, Lowell E.: The Performance of Conical Supersonic Scoop Inlets on Circular Fuselages. NACA RM L53I14a, 1953.

[redacted]

5. Campbell, Robert C.: Performance of Supersonic Ramp-Type Side Inlet with Combinations of Fuselage and Inlet Throat Boundary-Layer Removal. NACA RM E56A17, 1956.

6. Mitchell, Glenn A., and Campbell, Robert C.: Performance of a Supersonic Ramp-Type Side Inlet with Ram-Scoop Throat Bleed and Varying Fuselage Boundary-Layer Removal Mach Number Range 1.5 to 2.0. NACA RM E56I26, 1957.

7. Allen, John L.: Performance of a Blunt-Lip Side Inlet with Ramp Bleed, Bypass, and a Long Constant-Area Duct Ahead of the Engine: Mach Numbers 0.66 and 1.5 to 2.1. NACA RM E56J01, 1956.

[redacted]

DECLASSIFIED

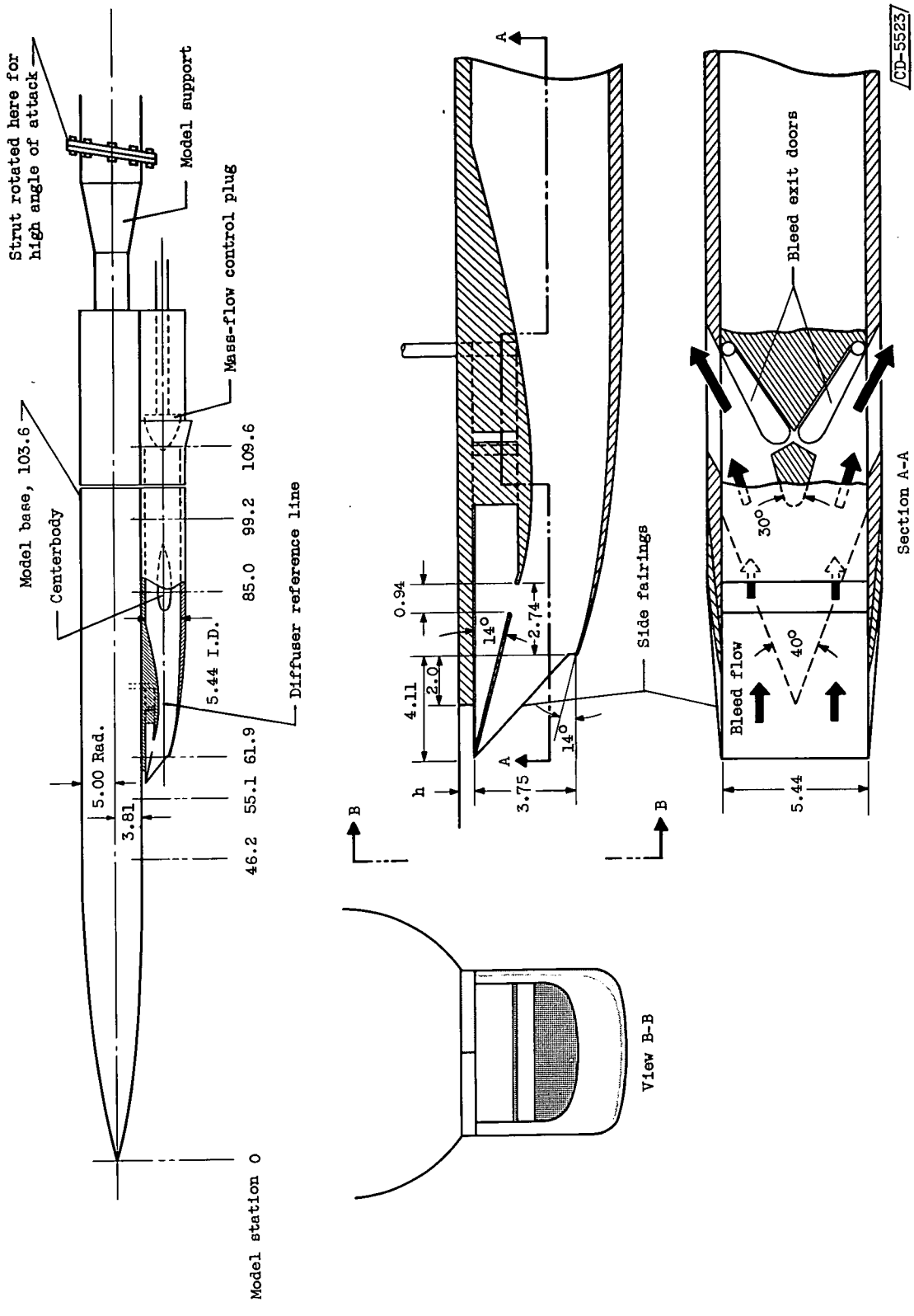

Figure 1. - Schematic drawing of model and inlet with flush slot bleed. (All dimensions in inches except where noted.)

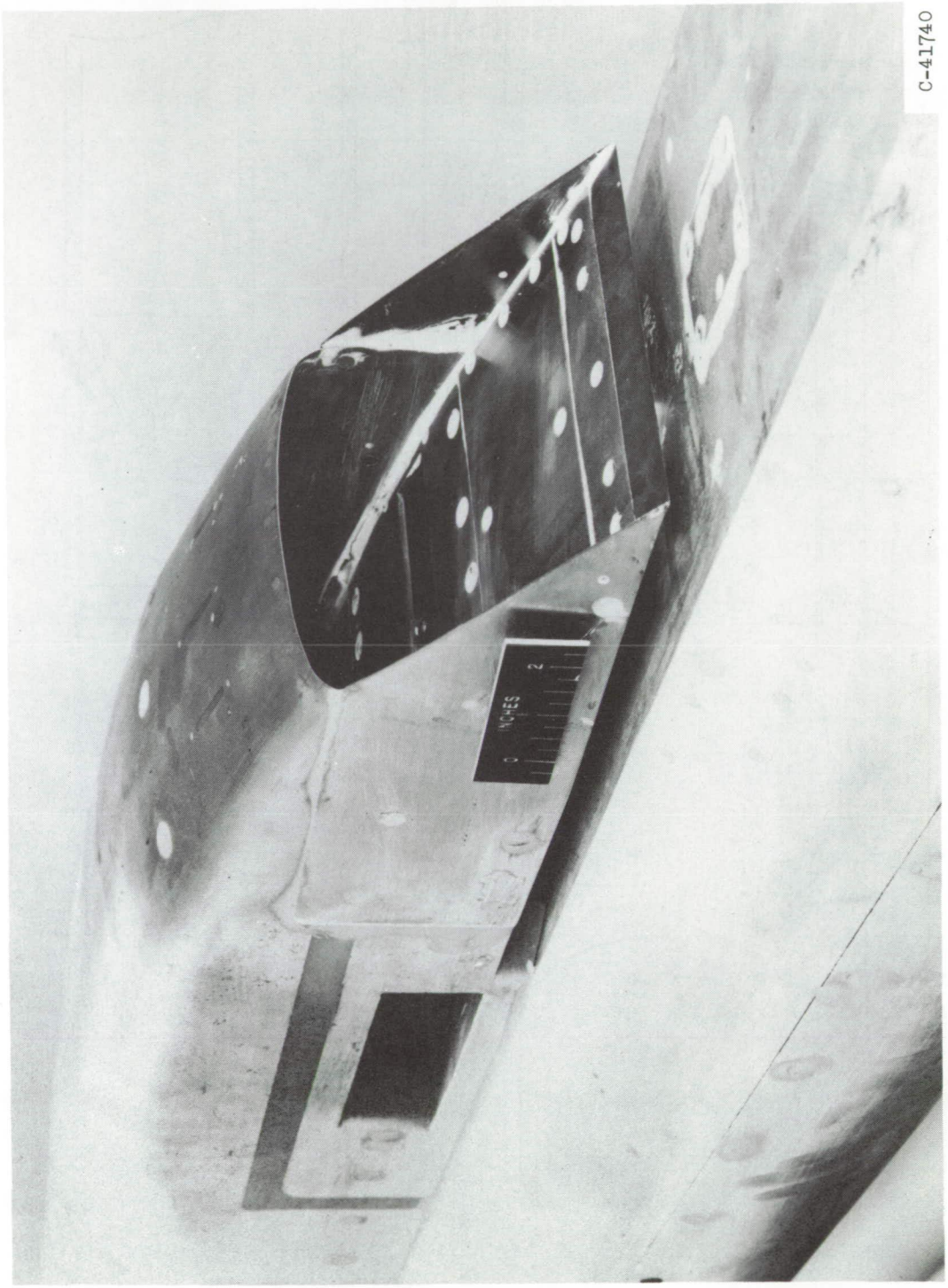

Figure 2. - Bottom inlet configuration. Flush slot bleed, 14° ramp inlet with side fairings.

DECLASSIFIED

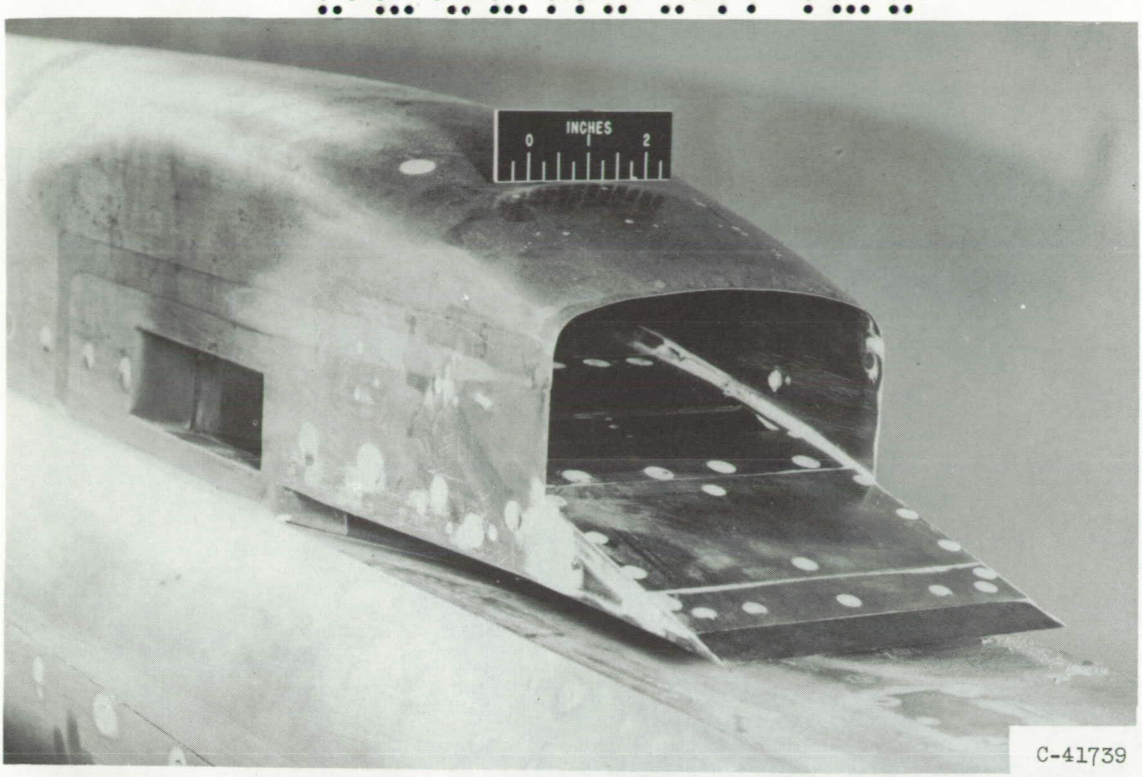

(a) Basic configuration. (No deflector plate.)

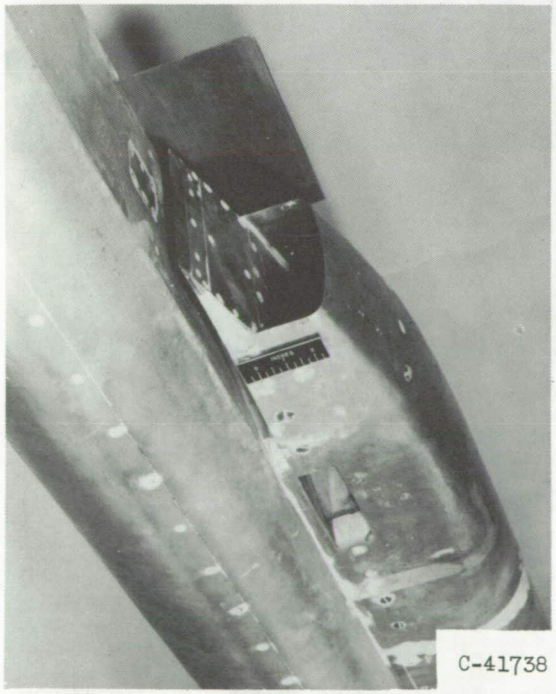

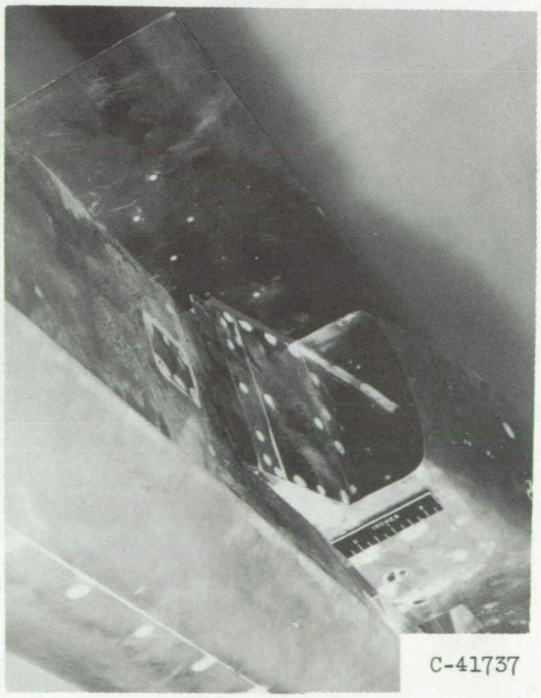

(b) Side inlet with short flow deflector plate. (c) Side inlet with long flow deflector plate.

Figure 3. - Side inlet configurations. Flush slot bleed, 14° ramp without side fairings.

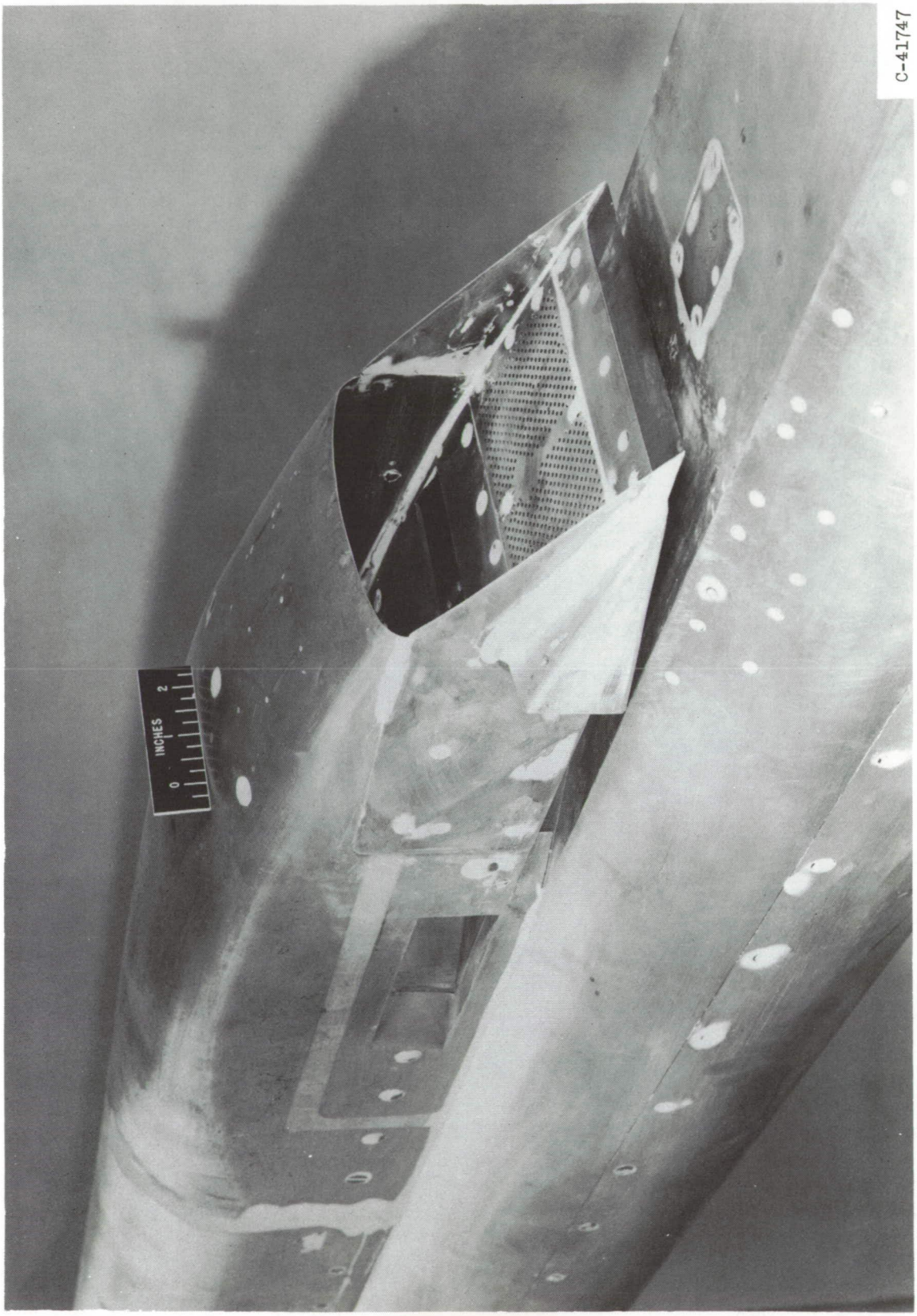

(a) Basic configuration. (Flat approach.)

Figure 4. - Top inlet configurations. Flush slot bleed and ramp perforations, 14° ramp inlet with side fairings.

DECLASSIFIED

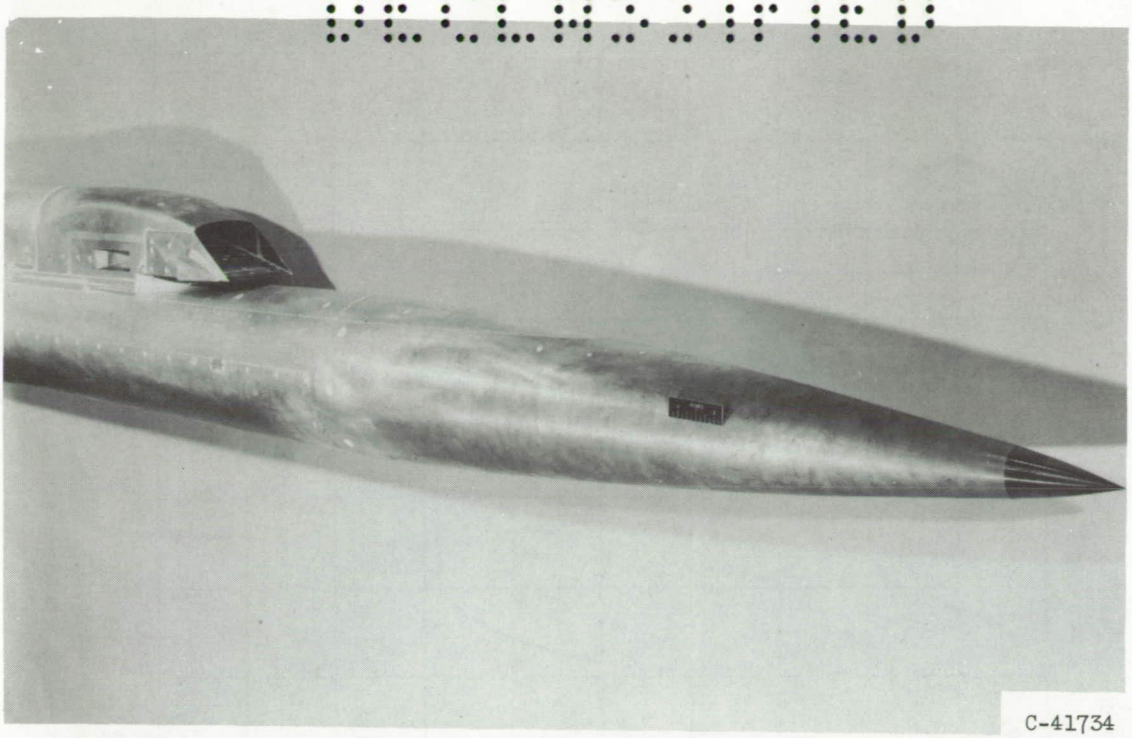

C-41734

(b) With rounded approach.

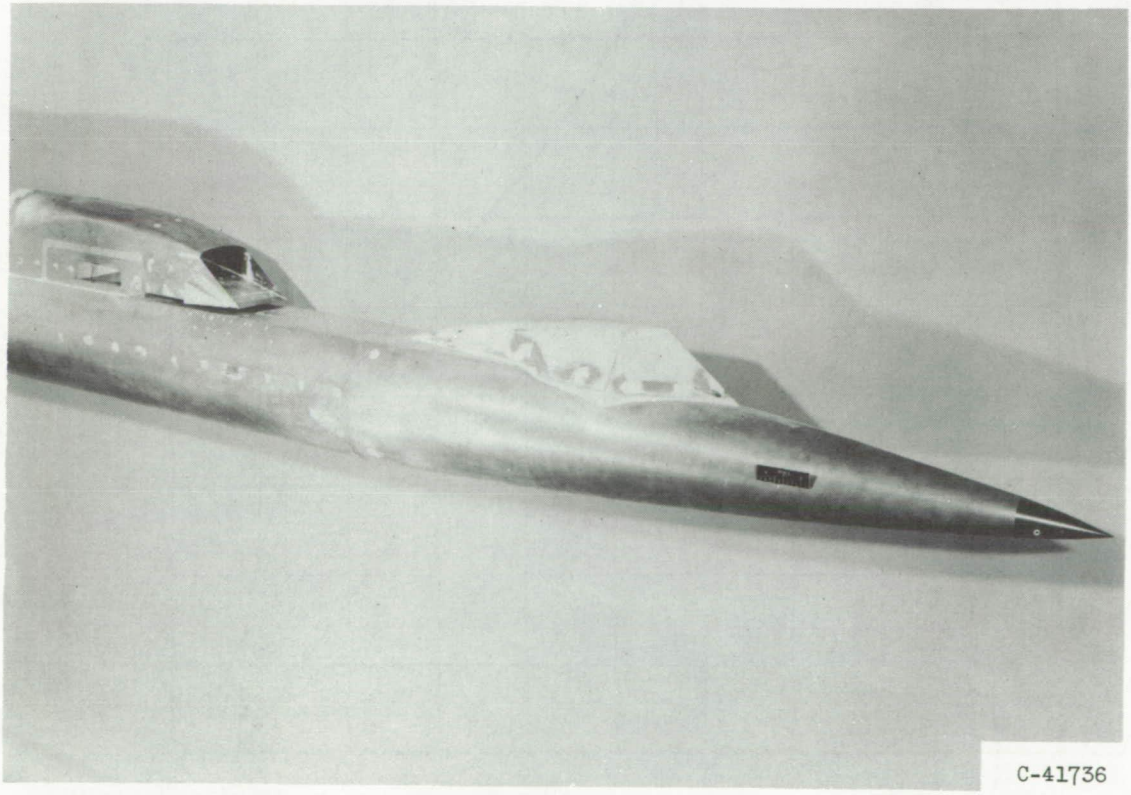

C-41736

(c) With canopy.

Figure 4. - Concluded. Top inlet configurations. Flush slot bleed and ramp perforations, 14° ramp inlet with side fairings.

DECLASSIFIED

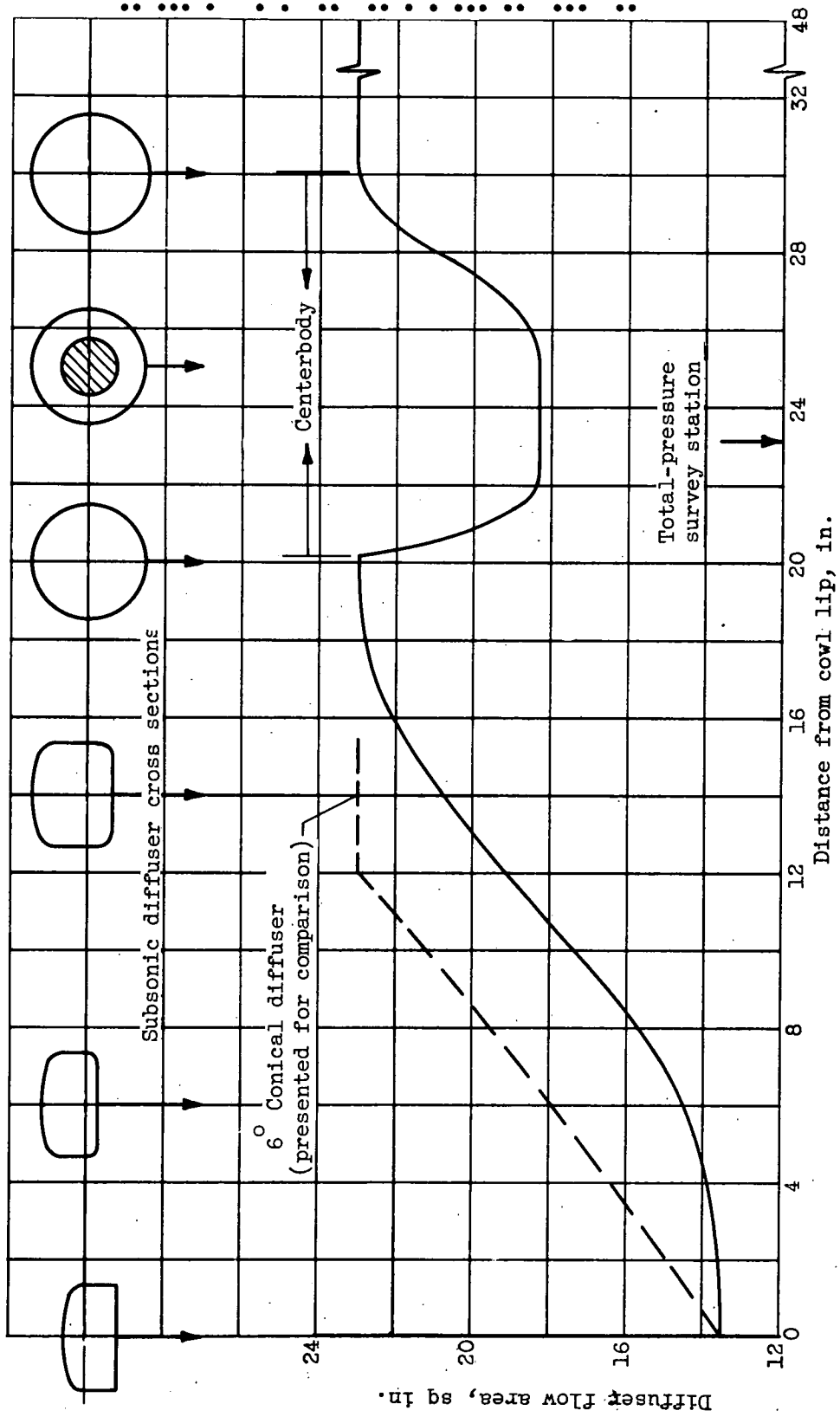

Figure 5. - Subsonic diffuser area variation. Inlet throat hydraulic diameter, 3.52 inches.

[redacted]

DECLASSIFIED
CONFIDENTIAL

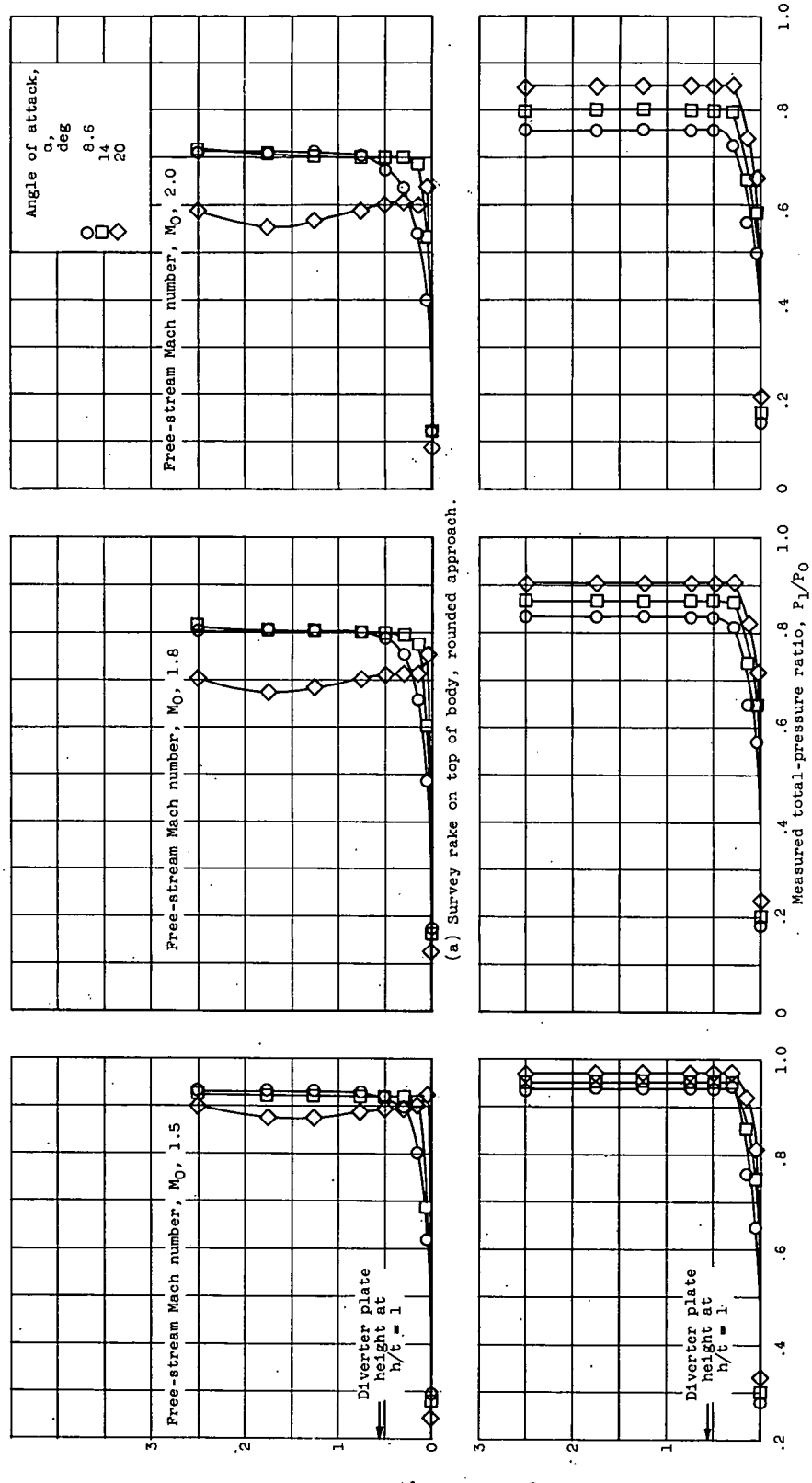

(a) Survey rake on top of body, rounded approach.

(b) Survey rake on bottom of body, flat approach.

Figure 6. - Radial total-pressure profiles ahead of inlet on inlet center plane.

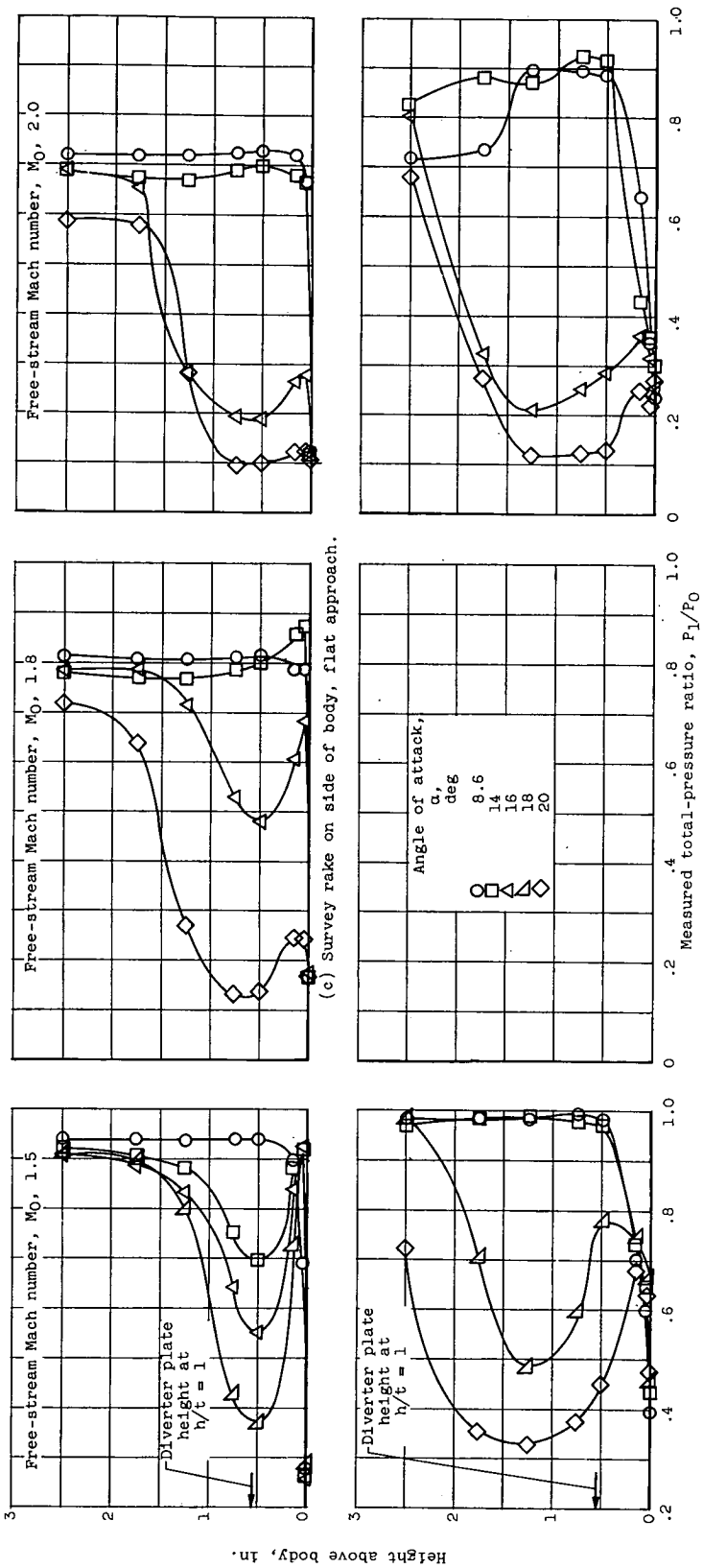

(c) Survey rake on side of body, flat approach.

(d) Survey rake on side of body, flat approach with long flow deflector plate.

Figure 6. - Concluded. Radial total-pressure profiles ahead of inlet on inlet center plane.

[redacted]

DECLASSIFIED

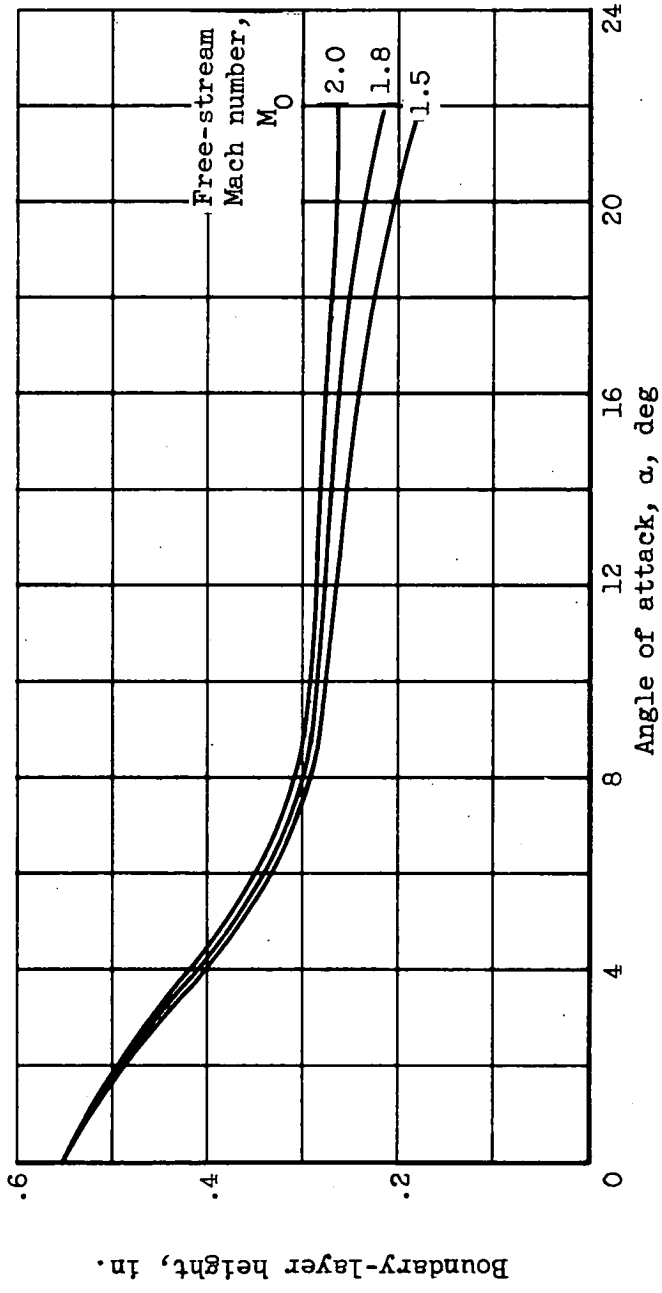

Figure 7. - Variation of boundary-layer thickness with angle of attack for bottom inlet location.

[redacted]

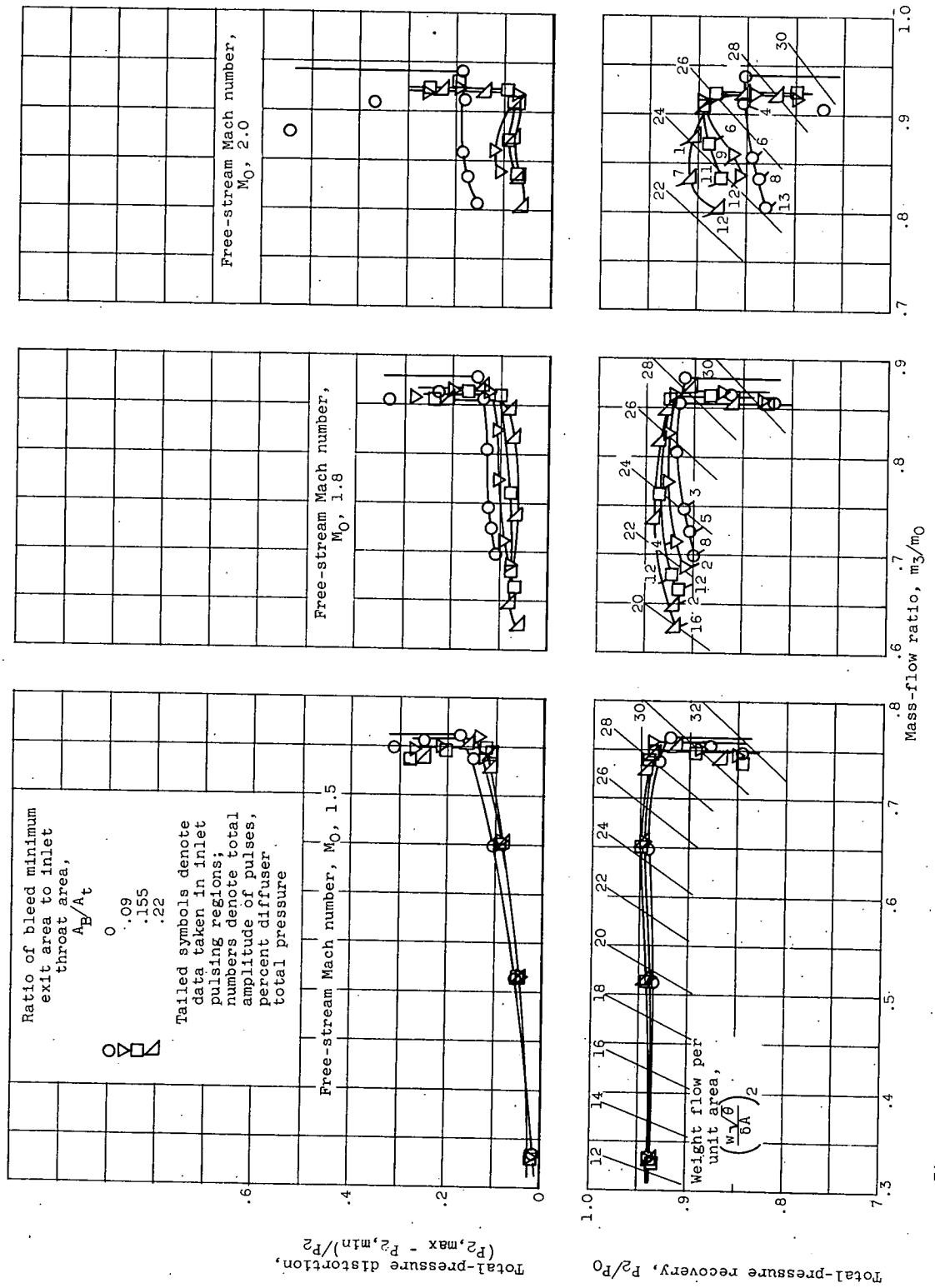

Figure 8. - Effect of inlet throat bleed on performance of bottom inlet. Angle of attack, 0°; fuselage diverter height parameter, 1.

DECLASSIFIED

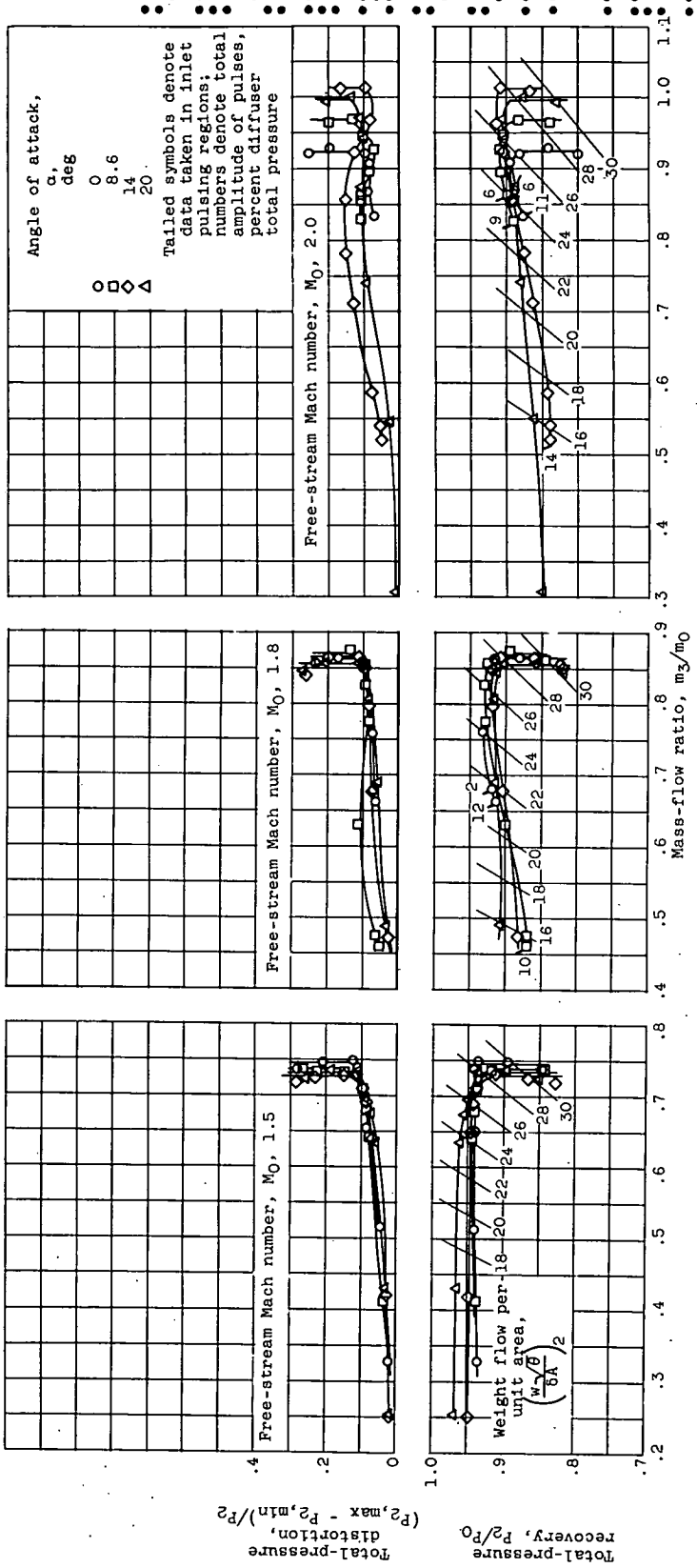

(a) Fuselage diverter height parameter, 1.

Figure 9. - Angle-of-attack performance for bottom inlet. Ratio of bleed minimum exit area to inlet throat area, 0.155.

CONFIDENTIAL

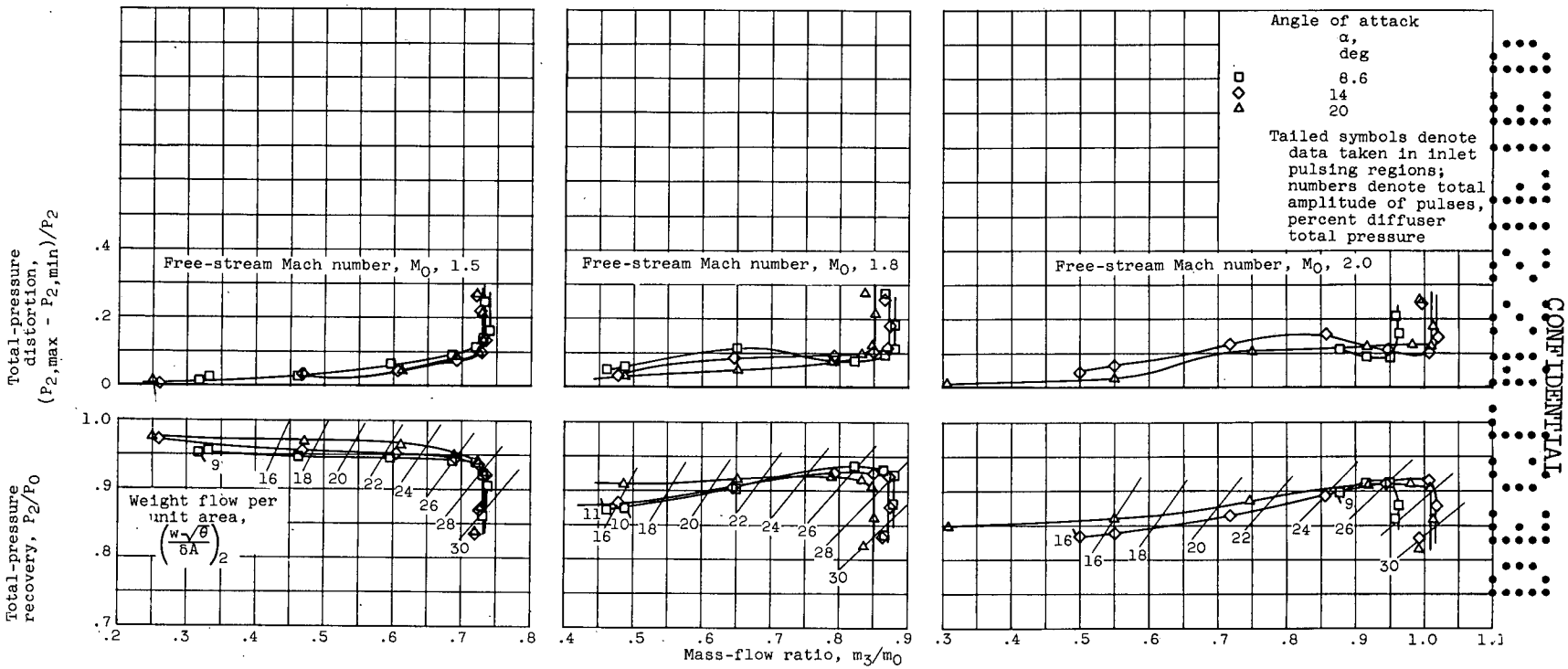

(b) Fuselage diverter height parameter, 1/3.

Figure 9. - Concluded. Angle-of-attack performance for bottom inlet. Ratio of bleed minimum exit area to inlet throat area, 0.155.

CONFIDENTIAL

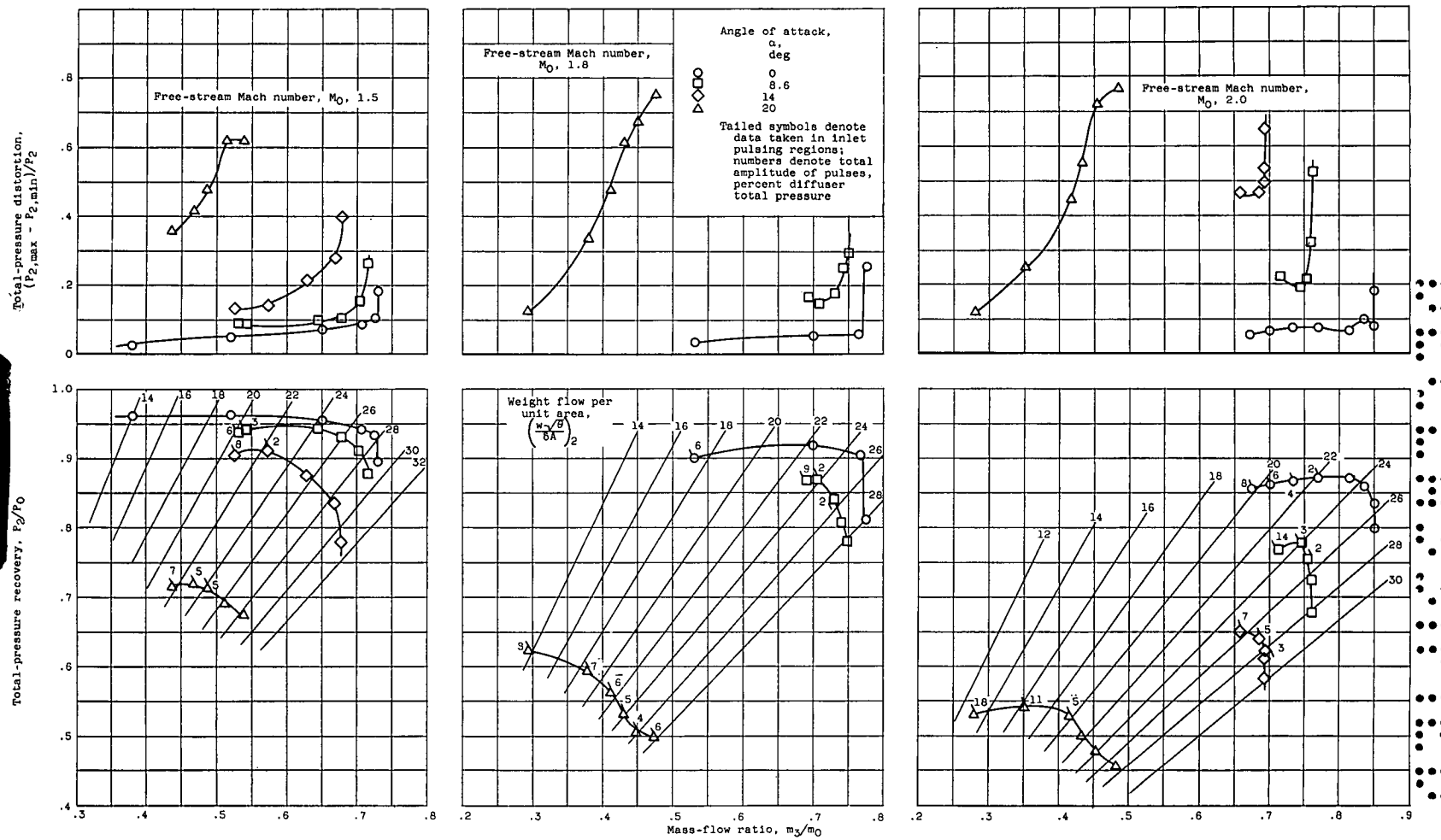

(a) Basic side inlet configuration (no deflector plate).

Figure 10. - Angle-of-attack performance for side inlet configurations. Ratio of bleed minimum exit area to inlet throat area, 0.155; fuselage diverter height parameter, 1.

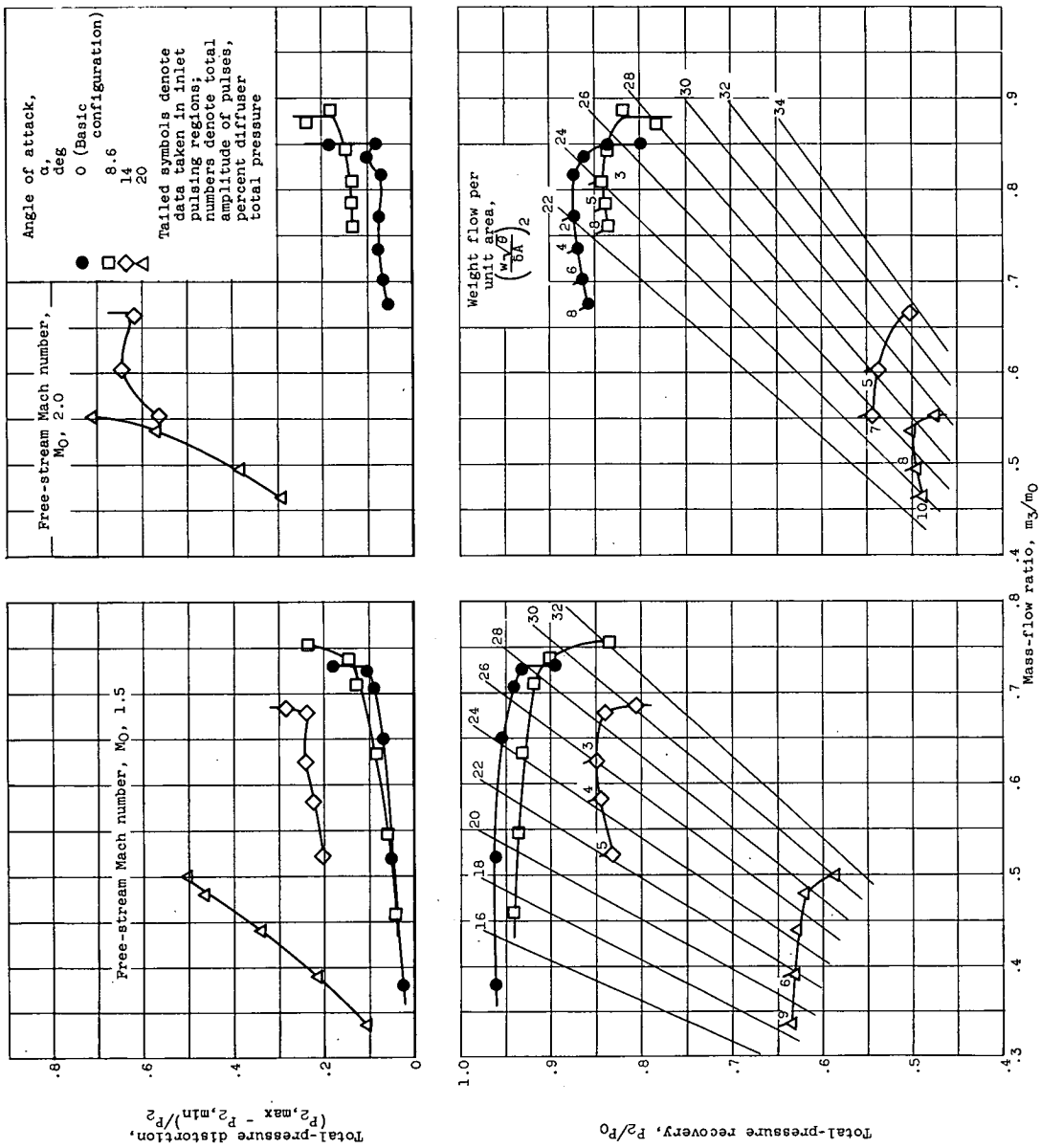

(b) Side inlet with short deflector plate.

Figure 10. - Continued. Angle-of-attack performance for side inlet configurations. Ratio of bleed minimum exit area to inlet throat area, 0.155; fuselage diverter height parameter, 1.

DECLASSIFIED

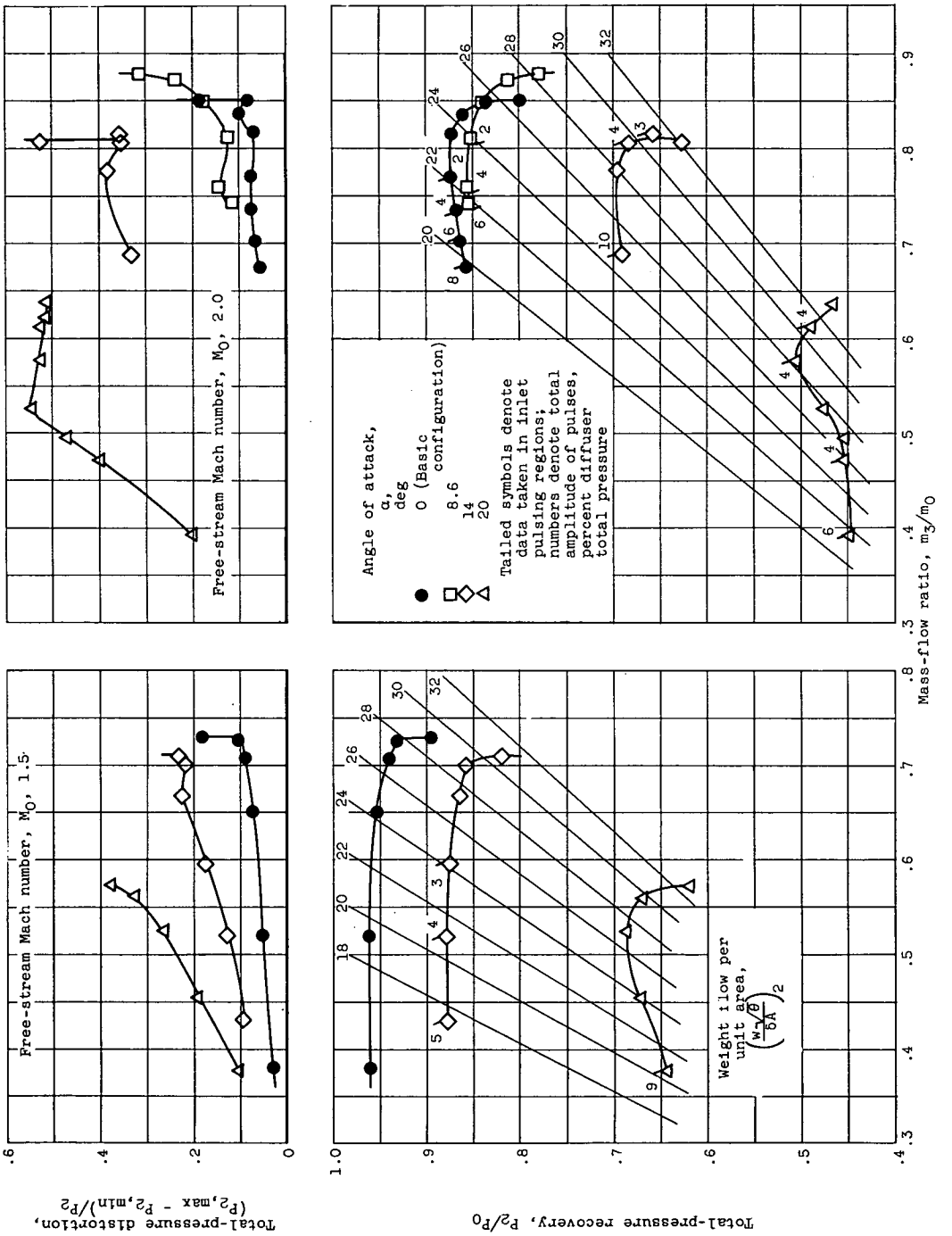

(c) Side inlet with long deflector plate.

Figure 10. - Concluded. Angle-of-attack performance for side inlet configurations. Ratio of bleed minimum exit area to inlet throat area, 0.155; fuselage diverter height parameter, 1.

[redacted]

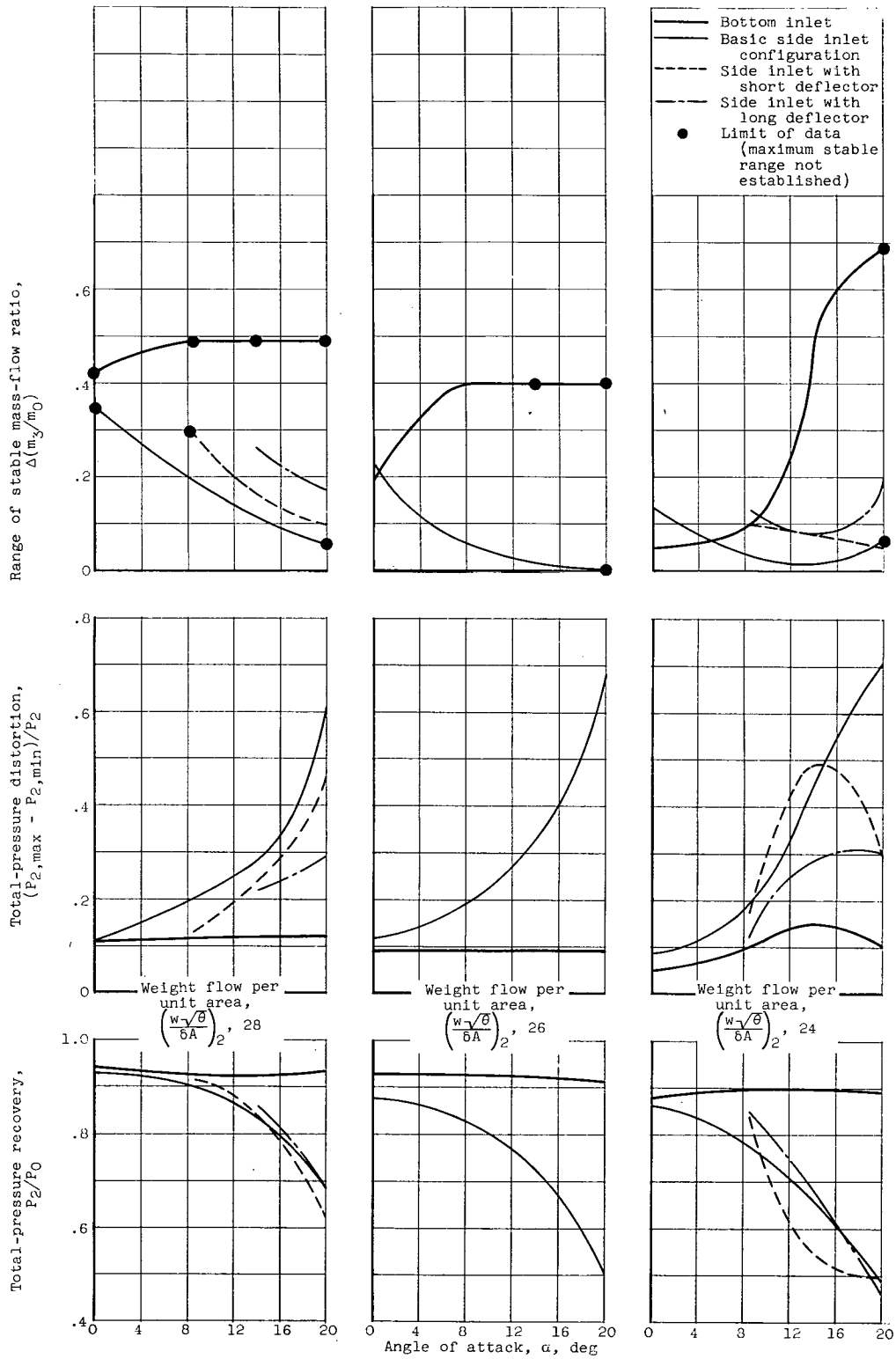

(a) Free-stream Mach number, 1.5. (b) Free-stream Mach number, 1.8. (c) Free-stream Mach number, 2.0.

Figure 11. - Summary of side inlet performance.

[redacted]

DECLASSIFIED

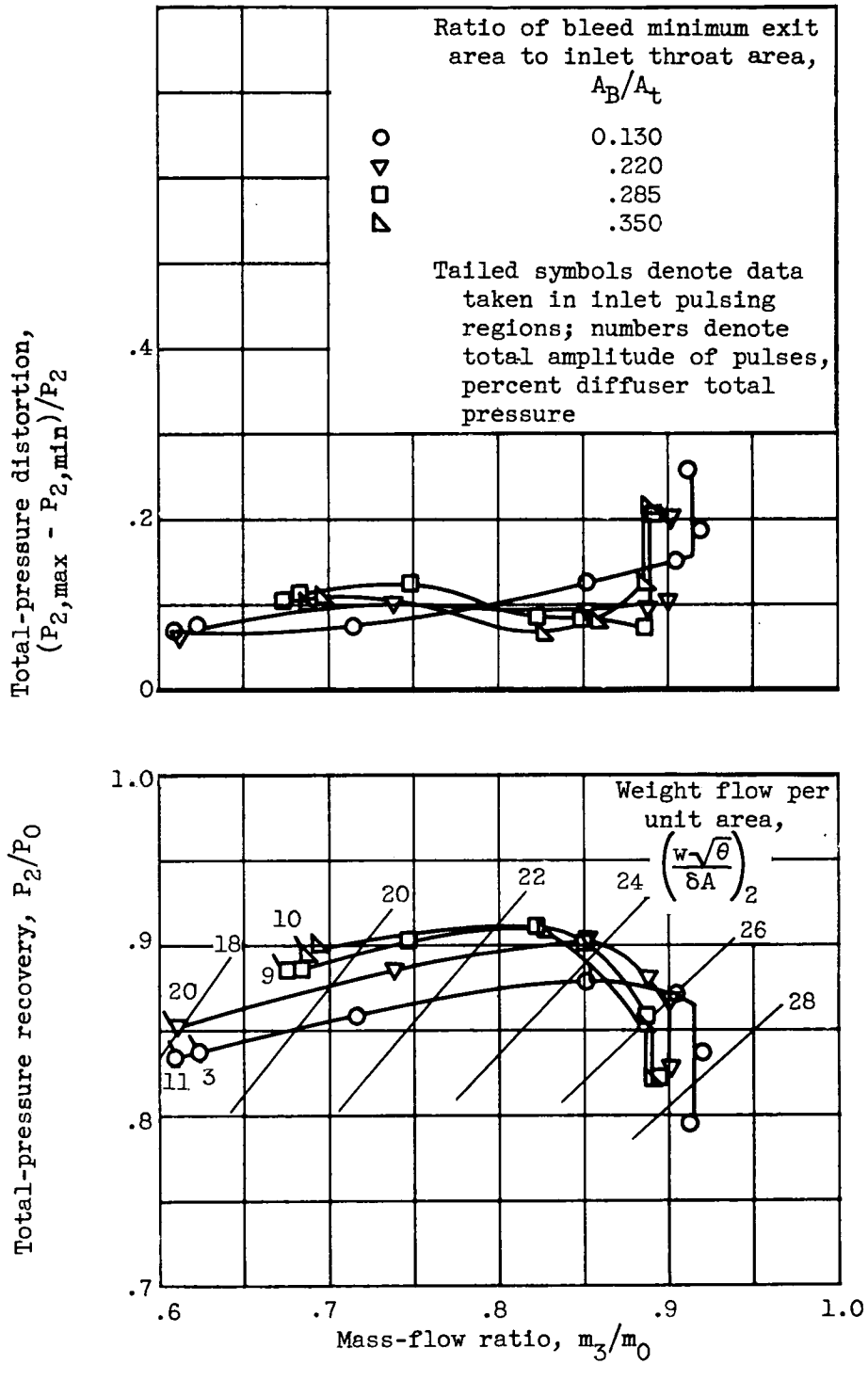

Figure 12. - Effect of inlet throat bleed on performance of top inlet. Free-stream Mach number, 2.0; angle of attack, 0°; fuselage diverter height parameter, 1.

[redacted]

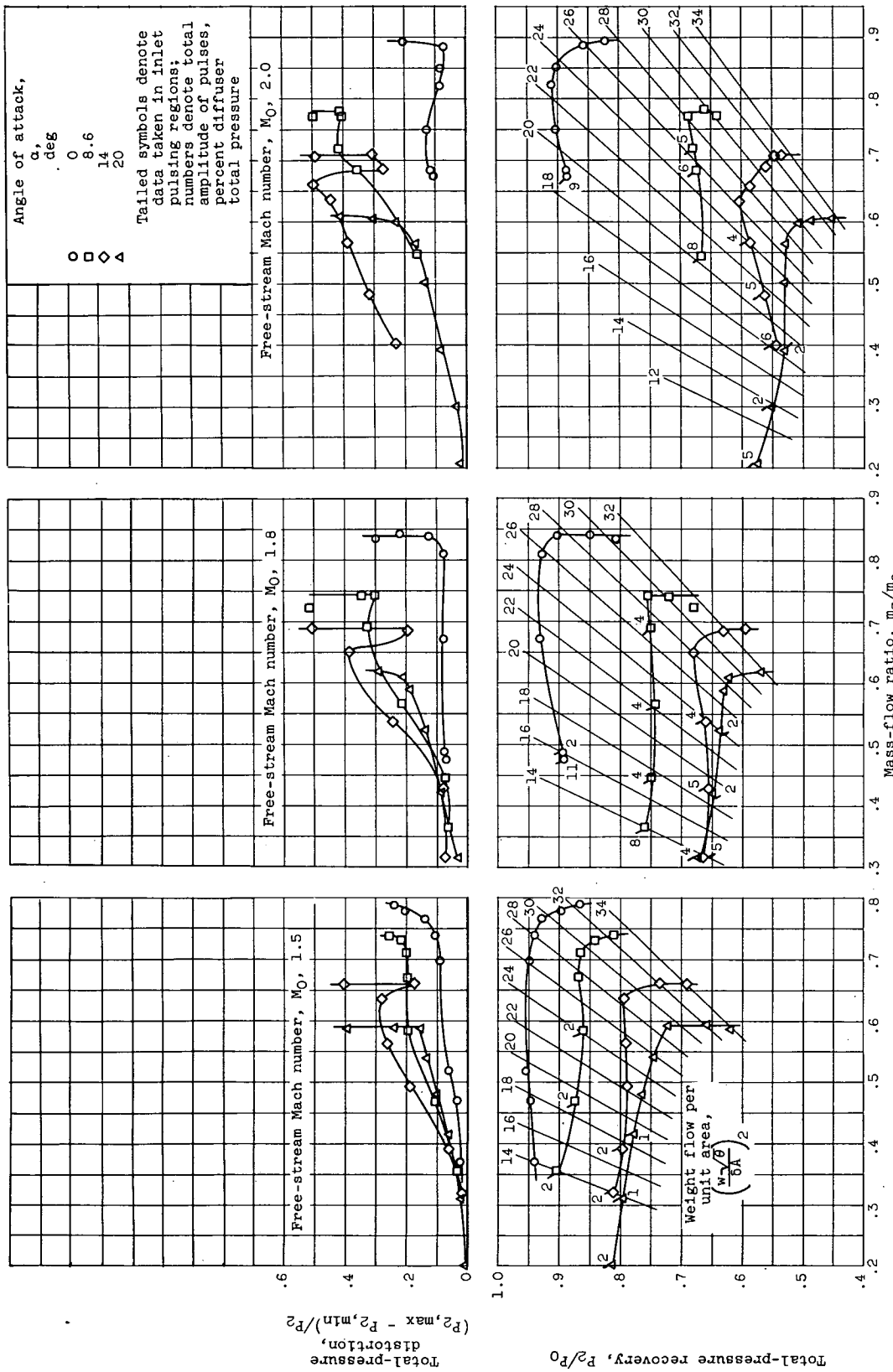

(a) Basic top inlet configuration, flat approach. Ratio of bleed minimum exit area to inlet throat area, 0.285.

Figure 13. - Angle-of-attack performance for top inlet configurations. Fuselage diverter height parameter, 1.

DECLASSIFIED

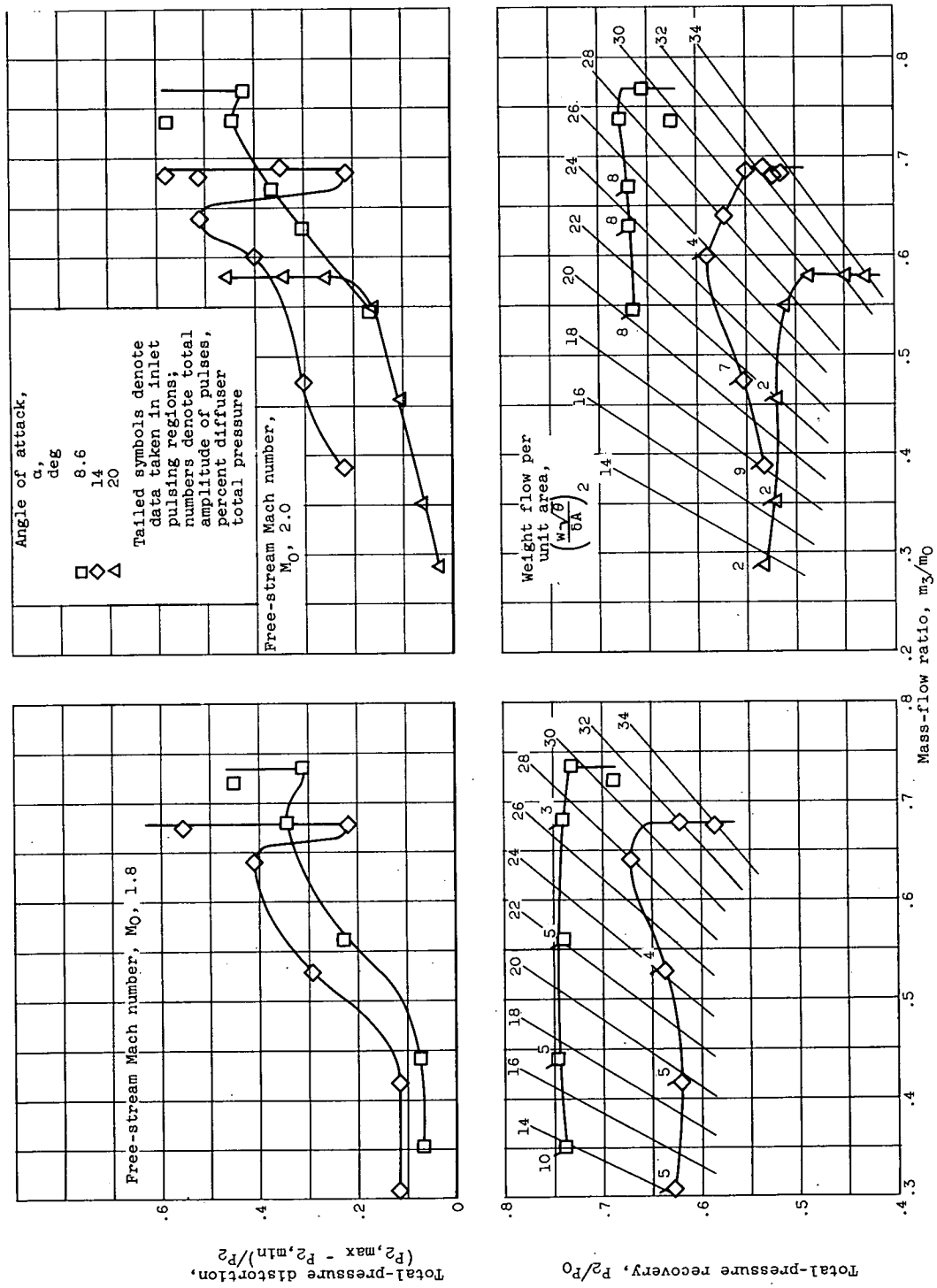

(b) Top inlet, flat approach. Ratio of bleed minimum exit area to inlet throat area, 0.595.

Figure 13. - Continued. Angle-of-attack performance for top inlet configurations. Fuselage diverter height parameter, 1.

[redacted]

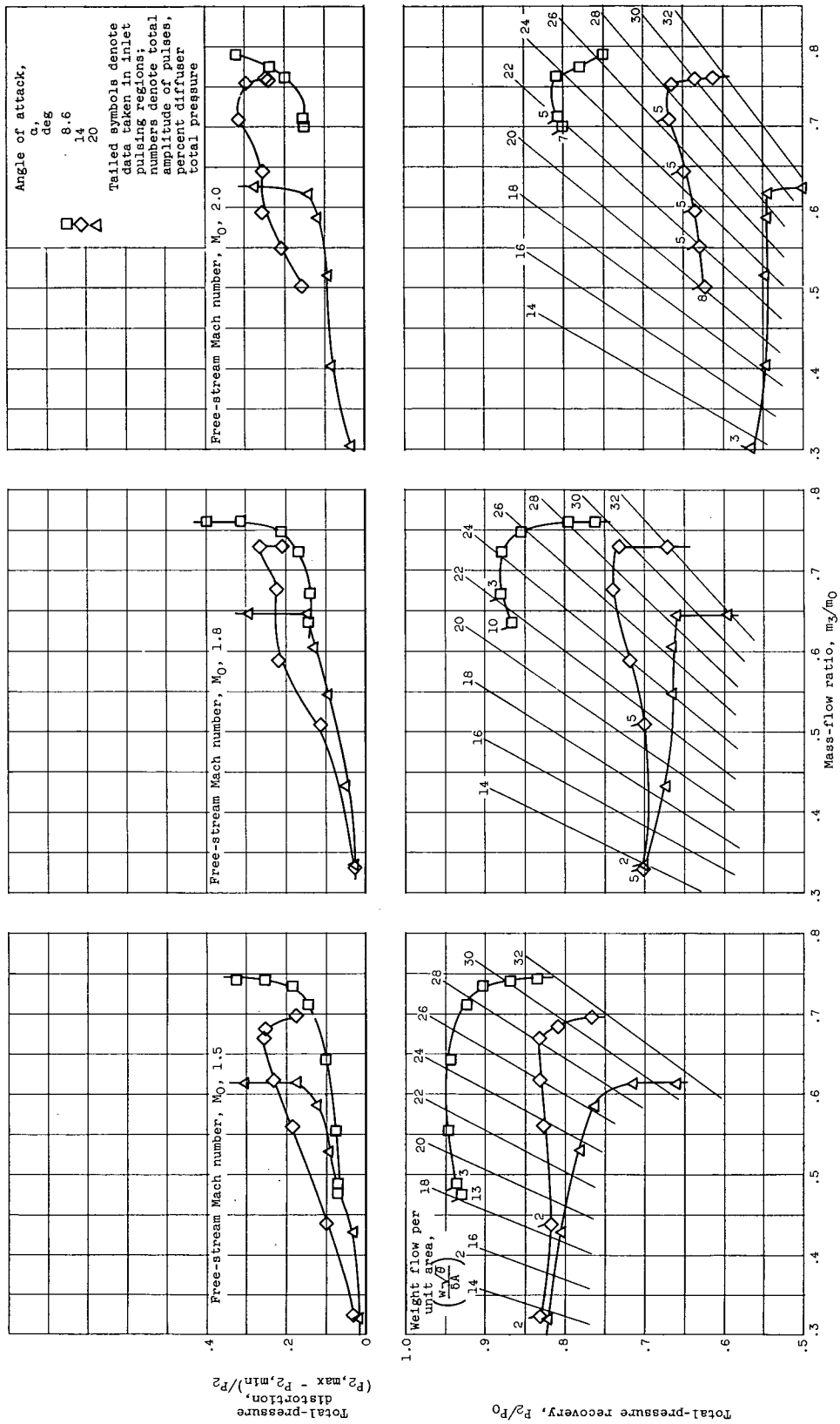

(c) Top inlet with rounded approach. Ratio of bleed minimum exit area to inlet throat area, 0.285.

Figure 13. - Continued. Angle-of-attack performance for top inlet configurations. Fuselage diverter height parameter, 1.

[redacted]

DECLASSIFIED

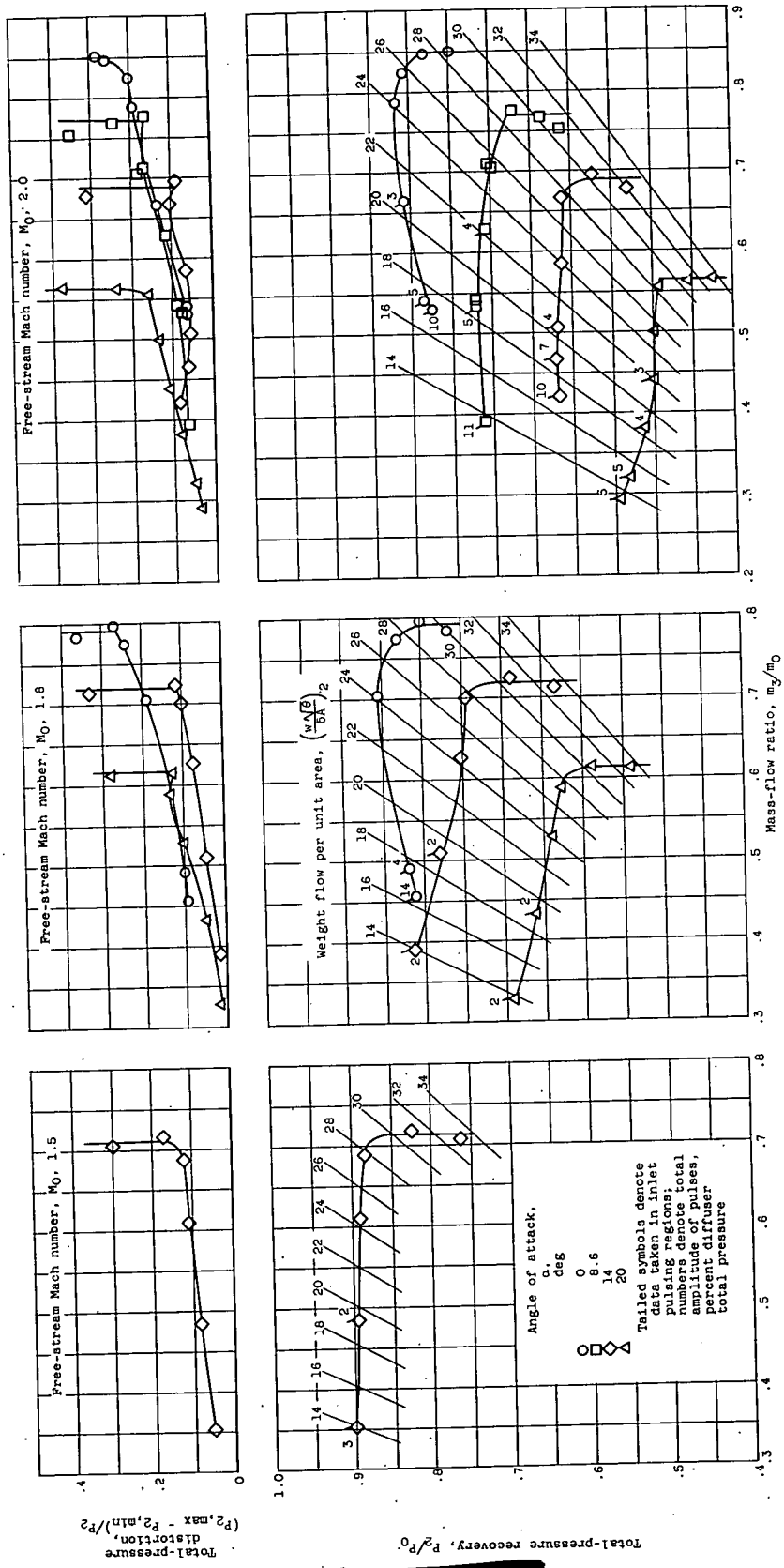

(d) Top inlet with canopy, flat approach. Ratio of bleed minimum exit area to inlet throat area, 0.285.

Figure 13. - Concluded. Angle-of-attack performance for top inlet configurations. Fuselage diverter height parameter, 1.

[redacted]

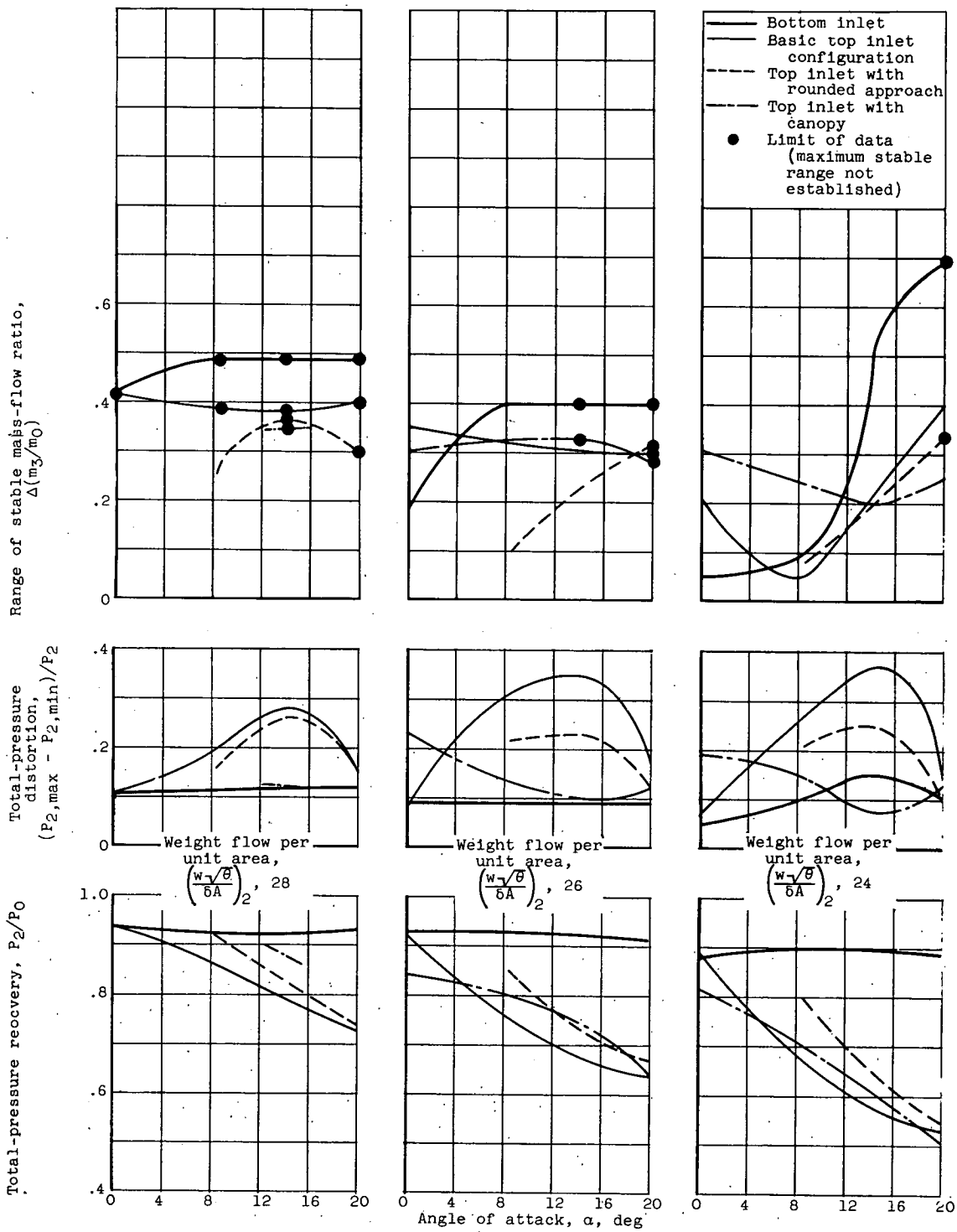

(a) Free-stream Mach number, 1.5. (b) Free-stream Mach number, 1.8. (c) Free-stream Mach number, 2.0.

Figure 14. - Summary of top inlet performance.

[redacted]

CONFIDENTIAL

DECLASSIFIED

CONFIDENTIAL